

NYCTEREUTES (MAMMALIA, CARNIVORA, CANIDAE) FROM LAYNA AND THE EURASIAN RACCOON-DOGS: AN UPDATED REVISION

SAVERIO BARTOLINI LUCENTI^{1,2}, LORENZO ROOK² & JORGE MORALES³

¹Dottorato di Ricerca in Scienze della Terra, Università di Pisa, Via S. Maria 53, 56126 Pisa, Italy

²Dipartimento di Scienze della Terra, Università di Firenze, Via G. La Pira 4, 50121 Firenze, Italy

³Departamento de Paleobiología. Museo Nacional de Ciencias Naturales, CSIC. C/ José Gutiérrez Abascal, 2, 28006 Madrid, Spain.

To cite this article: Bartolini Lucenti S., Rook L. & Morales J. (2018) - *Nyctereutes* (Mammalia, Carnivora, Canidae) from Layna and the Eurasian raccoon-dogs: an updated revision *Riv. It. Paleontol. Strat.*, 124(3): 597-616.

Keywords: Taxonomy; Canidae; Europe; Pliocene; *Nyctereutes*.

Abstract. The Early Pliocene site of Layna (MN15, ca 3.9 Ma) is renowned for its record of several mammalian taxa, among which the raccoon-dog *Nyctereutes donnezani*. Since the early description of this sample, new fossils of raccoon-dogs have been discovered, including a nearly complete cranium. The analysis and revision here proposed, with new diagnoses for the identified taxa, confirm the attribution of the majority of the material to the primitive taxon *N. donnezani*, enriching and clarifying our knowledge of the cranial and postcranial morphological variability of this species. Nevertheless, the analysis also reveals the presence in Layna of some specimens with strong morphological affinity to the derived *N. megamastoides*. The occurrence of such a derived taxon in a rather old site, has critical implications for the evolutionary history and dispersal pattern of these small canids. For instance, it reconciles the Western European and Asian records. Formerly, it was commonly thought that the evolutionary pattern of Early Pliocene raccoon-dogs in Europe was substantially different from the Asian one, where the advanced *N. sinensis* and the primitive *N. tingi* apparently coexisted in the same sites; conversely, Europe was characterized by the occurrence of the single species *N. donnezani*. Our recognition of a derived taxon in the MN15 zone suggests the existence of similar ecological dynamics at the two extremes of the paleobiogeographic range of the genus (i.e., across the entire Eurasia).

INTRODUCTION

The Western European record of the genus *Nyctereutes* is renowned since the first half of the XIX Century. Indeed, raccoon-dogs represent important elements of Eurasian fossil faunas from the late Ruscinian up to the middle-late Villafranchian, as evidenced by the discoveries in several localities. Although nowadays the genus is composed of a single species, *Nyctereutes procyonoides* (Gray, 1834), up to ten fossil species have been described, and three of them come from Western Europe. The earliest taxon in Eurasia is *Nyctereutes tingi* Tedford & Qiu, 1991 from the Early Pliocene of the Yushe Basin (China). From the same area another species comes, that is *Nyctereutes sinensis* (Schlosser, 1903), which possesses peculiar features compared to the previous taxon (e.g., prominent subangular lobe, larger angular pro-

cess). The extant raccoon-dog is an opportunistic feeder that possesses several cranial and dentognathic specialization to a diet composed of a great variety of food items (Ward & Wurster-Hill 1991). Its main adaptations lie in numerous cranial and dentognathic features that improve the efficiency in the chewing process while feeding; among them, the development of the subangular lobe, the enlargement of the angular process, and the morphology of the upper molars. These features characterize raccoon-dogs throughout their evolutionary history and are particularly evident in the extant *N. procyonoides*. Soria & Aguirre (1976) were among the first to study critically fossil raccoon-dogs considering their complete record, taking into account the interspecific and intraspecific variability and the principal features of the fossil and of the extant species of the genus. They acknowledged the peculiarity of *N. procyonoides* and identified in certain mandibular and dental characters (i.e., depth of mandible cor-

Received: July 14, 2018; accepted: October 05, 2018

pus; morphology of the angular region; inclination of the ascending ramus; the premolars and molars morphology) the key features for the evolutionary differentiation of raccoon-dogs. Specifically, Soria & Aguirre (1976) outlined the first pattern of morphological affinity and relation between the species of *Nyctereutes*. This was achieved thanks to the recognition of “primitive” taxa (with e.g., poorly developed subangular lobe and elongated and buccolingually narrow premolars) and of “derived” taxa (in which e.g., there is a marked development of the subangular lobe and stouter premolars) that resemble the extant *N. procyonoides* (Soria & Aguirre 1976). Since this pivotal work, in the scientific literature on *Nyctereutes*, this terminology was used by several scholars to discuss the morphological set of features a fossil raccoon-dog possessed (Ficcarelli et al. 1984; Tedford & Qiu 1991; Argant 2004; Monguillon et al. 2004), with no explicit reference to the phylogenetic relationship of a taxon. In this work, the terminology follows the same intent: express the degree development of the set of morphological features, without implying any evolutionary inference. In this terms, *N. tingi* can be considered a rather primitive taxon, for the absence and/or incipient development of these characters (as also noted by Tedford & Qiu 1991), whereas *N. sinensis* is rather derived, resembling the morphologies of the living raccoon-dog.

On the other side of Eurasia, the oldest form described in Western Europe is *Nyctereutes donnezani* (Depéret, 1890), first discovered in Perpignan (France) and then reported in other localities such as La Gloria 4 (Spain; Alcalá-Martínez 1994). These sites are referred to the Early Pliocene, MN14-15 (around 4 Ma) (Domingo et al. 2013; Clauzon et al. 2015). Since its first description, *N. donnezani* has been regarded as a primitive species, for the morphological similarities with the early and roughly coeval *N. tingi*. Around 3 Ma *Nyctereutes megamastoides* (Pomel, 1842) appeared in Europe, where its earliest record is in Italy (Bartolini Lucenti 2017). The species soon spread all over Europe, from Spain (Morales 2016) to Greece (Koufos 2014) and Georgia (Rook et al. 2017). Commonly, the origin of this Eurasian species has been related to the primitive *N. donnezani* from which anagenetically *N. megamastoides* would have evolved (Soria & Aguirre 1976). The strongly derived morphology of the latter taxon (e.g., development of a large subangular lobe and the deep

angular process) resembles that of *N. sinensis* and *N. procyonoides*. For this reason, several authors (e.g., Soria & Aguirre 1976; Tedford & Qiu 1991) deemed plausible the hypothesis that *N. sinensis* and *N. megamastoides* might represent a single species with a very wide paleobiogeographic range. Nevertheless, beyond similarities, there are several features that differentiate *N. megamastoides* from the Chinese species (Rook et al. 2017). The *N. megamastoides* sample from the French site of St. Vallier, firstly described by Viret (1954), was later referred to the subspecies, namely *Nyctereutes megamastoides vulpinus* Soria & Aguirre, 1976, on the basis of some differences (i.e., relatively longer upper and lower premolars and lower carnassial and reduced m2) with the typical morphology of *N. megamastoides*. More recently, Monguillon et al. (2004) reviewed the material of raccoon-dog of St. Vallier. These authors deemed the difference with the species *N. megamastoides* too important to be regarded as intraspecific variability and elevated the taxon to the rank of species, i.e. *N. vulpinus*, an attribution also followed in recent papers (e.g., Geraads et al. 2010; Rook et al. 2017; Bartolini Lucenti 2018).

Soria & Aguirre (1976) first described the *Nyctereutes* sample from Layna and attributed it to *N. donnezani*. Here, we describe new raccoon-dog material (among which a nearly complete cranium) from the same site and report the first diagnoses for both *N. donnezani* and *N. megamastoides*. Furthermore, we discuss the Layna record in the framework of the evolutionary history of *Nyctereutes* in Eurasia and of the most recent studies of this group of canids.

GEOLOGICAL SETTING

The karstic site of Layna (Soria Province, Spain) is located in the NW area of the Castilian Range (Iberian Chain), near the homonymous village (Fig. 1). It was the first Spanish paleontological site declared as a National Paleontological Reserve. The fossils occur in a karstic deposit developed in the lower Lias unit known as the Carniolas Formation that in the studied area, is superposed on the erosional surface of the so-called Parameras de Molina (Aguirre et al. 1974). The richness and diversity of the vertebrate fauna, most particularly of the small mammal species, are one of the most remarkable of the Spanish paleontological record. Although

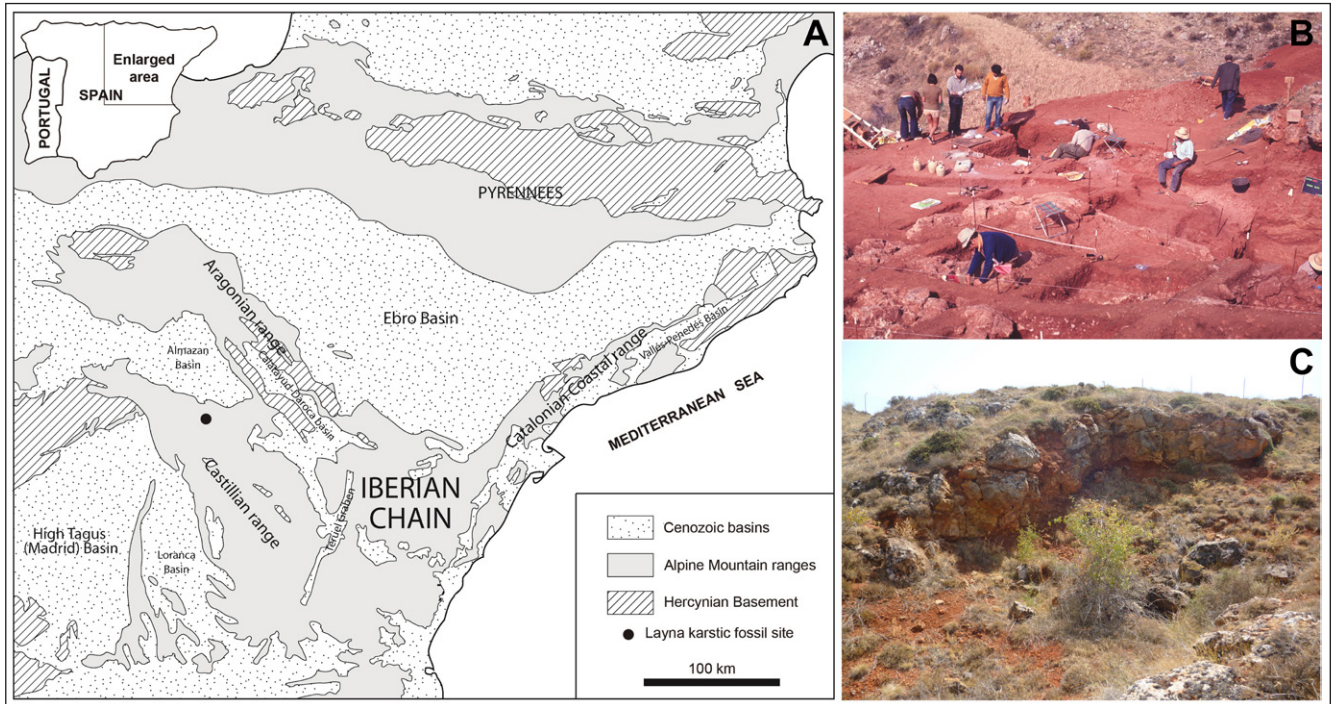


Fig. 1 - Geographic location and photos of the Layna fossil vertebrate site. A. Position of the site with the schematic representation of the enlarged area in the Iberian Peninsula on top left. B-C. Pictures of the First systematic excavation of Layna locality, directed by Prof. Emiliano Aguirre in 1972 (B) and the site nowadays (C) (2012). Photo credits: B, Prof. E. Aguirre; C, Prof. J. Morales.

there are many different types of sedimentary infillings, the recorded faunal remains, in the present state of our knowledge, seem to be homogeneous. The age of the site, based on the rodent remains, is Ruscinian (MN15; Early Pliocene) (López-Martínez 1989; Sesé 2006). Preliminary magnetostratigraphic studies suggested a normal polarity within the Gauss Chron (Hoyos et al. 1987). More recently, other interpretations of the faunal assemblage has yielded an early age of 3.91 Ma (Domingo et al. 2007, 2013). A further important point about Layna is that it preserves evidence of occupation not only by predatory birds but also by hyenas. This allows taphonomic interpretations of great interest (Aguirre et al. 1981; Pérez & Soria 1989-90).

MATERIALS AND METHODS

The present study is based on the comparative morphological analysis of the *Nyctereutes* record from Layna. The considered fossils are housed at the Museo Nacional de Ciencias Naturales. As comparative fossil material, we studied the collections of the Geology and Paleontology section of the Museum of Natural History of Florence, of the Geor-

gian National Museum in Tbilisi, of the Hungarian Museum of Natural History in Budapest, of the Musée des Confluences in Lyon, of the Université Claude Bernard de Lyon, of the American Museum of Natural History in New York and of the Musée National d'Histoire Naturelle in Paris. We also reviewed the relevant literature on Plio-Pleistocene raccoon-dogs (Martin 1971; Soria & Aguirre 1976; Torre 1979; Tedford & Qiu 1991; Monguillon et al. 2004; Bartolini Lucenti 2017; Rook et al. 2017). The fossil comparative sample includes specimens of *N. donnezani* from La Gloria 4 and Perpignan; *Nyctereutes* sp. from Çalta; *N. megamastoides* from the Lower Valdarno Basin, Kvabebi, Villarroya, Dafnero, Perrier-Les Etouaires; *N. vulpinus* from St. Vallier; *N. sinensis* from the Yushe Basin and Nihewan Basin, and *N. tingi* from the Yushe Basin.

The extant comparative sample includes specimens of *N. procyonoides*, *Vulpes vulpes* (Linnaeus, 1758), *Vulpes lagopus* (Linnaeus, 1758) and *Cerdocyon thous* Smith, 1839 housed in the MZUF and AMNH.

Craniodental and postcranial measurements were taken to the nearest 0.1 mm with a digital caliper following Driesch (1976).

Statistical analyses were performed using PAST software ver. 3.08 (Hammer et al. 2001;

Hammer 2016). We further clarified the specific attribution of *Nyctereutes* material by comparing the sample from Layna with other Eurasian Plio-Pleistocene and extant species of the genus by means of log-ratio diagram (Simpson 1941; Simpson et al. 1960). With the log-transformed mean value of each variable for every species, this graph estimates the difference between these values and a selected species, which constitutes the chosen comparative baseline. The dental variables selected are the P3 length, the P4-M2 length and width for the upper teeth, while for the lower dentition the p3 length and the p4-m2 length and width. For our analyses, we selected the extant *N. procyonoides* as a reference baseline. We then plotted the following species: *N. megamastoides* from various European sites; *N. tingi* and *N. sinensis* from China; *N. vulpinus* from St. Vallery, and *N. donnezani* from Layna, Perpignan and La Gloria 4.

We used the molar ratio index (Asahara 2013) to investigate the dietary preferences of *N. donnezani* from Layna in comparison to some extant subspecies [i.e., *Nyctereutes procyonoides albus* (Hornaday, 1904) and *Nyctereutes procyonoides viverrinus* (Temminck, 1838)] and fossil species of this genus (data taken from Asahara & Takai 2016 and SBL personal data). The method described by Asahara (2013) consists in calculating the occlusal surface of the m1 and the m2, and then estimate the ratio between the two surfaces (i.e., m2/m1 score). In Canidae, this molar ratio proves to be related to the differences in diet (Asahara 2013, 2014; Asahara et al. 2016). After measuring the tooth length and width, we calculated the occlusal area following Kavanagh et al. (2007). We used these new scores to plot all the data in a biplot diagram of m1 occlusal surface versus m2/m1 score of each extant populations or fossil species to compare them with the results by Asahara & Takai (2016) and Bartolini Lucenti (in press).

Materials studied

Nyctereutes donnezani

Cranium and cranial fragments – MNCN-39920, left maxillary fragment with M1-M2; MNCN-62478, left maxillary fragment with P4; MNCN-62482, right maxillary fragment with P2; MNCN-62610, cranial fragment in sediment matrix; MNCN-63662, cranium with left I3-P2, P4-M2 and right I3-C1, P2, P4 and M2.

Upper teeth – MNCN-62599, left I2; MNCN-62600, left I3; MNCN-62494, left C1; MNCN-62496, right C1; MNCN-62483, right P3; MNCN-62479, left P4; MNCN-62480, right P4; MNCN-62491, right M1; MNCN-62493, left M2.

Mandible – MNCN-39916, right hemimandible with p2-

p3 and m1-m3; MNCN-39917, right hemimandible with p4-m2; MNCN-39919, right hemimandible with p4-m2; MNCN-62616, right hemimandible with m2; MNCN-62617, right hemimandible with p2; MNCN-62618, right hemimandible, edentulous; MNCN-62619, left hemimandible with m2; MNCN-62620, right hemimandible; MNCN-62621, right hemimandible with p1; MNCN-62625, right hemimandible fragment, edentulous; MNCN-62643, fragment of hemimandible ramus; MNCN-71082, right hemimandible fragment; MNCN-71083, right hemimandible, edentulous; MNCN-71087, right hemimandible with m1.

Lower teeth – MNCN-62602, left i1; MNCN-62598, left i2; MNCN-71086, left i2; MNCN-62597, left i3; MNCN-62495, right c1; MNCN-62497, right c1; MNCN-62651, right c1; MNCN-70008, left c1; MNCN-71085, right p3; MNCN-62519, right m1; MNCN-62520, right m1; MNCN-62608, left m1; MNCN-62609, right m1; MNCN-70007, left m3.

Postcranial elements – MNCN-62563, fragment of juvenile diaphysis; MNCN-62575, fragment of left scapula; MNCN-62576, fragment of right scapula; MNCN-62577, fragment of right scapula; MNCN-62632, fragment of left scapula; MNCN-62634, fragment of right scapula; MNCN-62635, fragment of right scapula; MNCN-62502, distal epiphysis of left humerus; MNCN-62503, proximal epiphysis and fragment of diaphysis of left humerus; MNCN-62603, fragment diaphysis of left humerus; MNCN-62604, distal epiphysis of right humerus; MNCN-62631, distal epiphysis of right humerus; MNCN-13651, proximal epiphysis of right radius; MNCN-13652, proximal epiphysis of right radius; MNCN-13654, distal epiphysis of left radius; MNCN-70904_1, distal epiphysis of left radius; MNCN-70904_2, fragment of distal epiphysis of right radius; MNCN-70905, distal epiphysis of left radius; MNCN-70906, proximal epiphysis of left radius; MNCN-70907, fragment of distal epiphysis of right radius; MNCN-62550, fragment of right ulna; MNCN-62551, fragment of left ulna; MNCN-62552, fragment of left ulna; MNCN-62553, fragment of right ulna; MNCN-62554, fragment of left ulna; MNCN-62555, fragment of right ulna; MNCN-62556, fragment of ulna; MNCN-62557, fragment of right ulna; MNCN-62622/549, fragment of right ulna; MNCN-62623, fragment of right ulna; MNCN-70006, fragment of left ulna; MNCN-62614, fragment of pelvis; MNCN-62615, fragment of right pelvis; MNCN-52972, right femur; MNCN-62473/75, proximal epiphysis of right femur; MNCN-62474, proximal epiphysis of right femur; MNCN-62476, proximal epiphysis of right juvenile femur; MNCN-62477, proximal epiphysis of right femur; MNCN-62558, distal epiphysis of left juvenile femur; MNCN-62559, distal epiphysis of left femur; MNCN-62560, distal epiphysis of right femur; MNCN-62561, distal epiphysis of right femur; MNCN-62562, fragment of distal epiphysis of femur; MNCN-62636, proximal epiphysis of left femur; MNCN-62637, distal epiphysis of left femur; MNCN-62638, proximal epiphysis of right femur; MNCN-62484, fragment of distal epiphysis of left tibia; MNCN-62485, distal epiphysis of right tibia; MNCN-62486, fragment of distal epiphysis of left tibia; MNCN-62487, distal epiphysis of right tibia; MNCN-62488, proximal epiphysis of left tibia; MNCN-62489, fragment of proximal epiphysis of left tibia; MNCN-62490, proximal epiphysis of left tibia; MNCN-62639, proximal epiphysis of left tibia; MNCN-70911, fragment of distal epiphysis of right tibia.

Nyctereutes cf. *megamastoides*

Cranium and cranial fragments – MNCN-39921, left maxillary fragment with P4-M1.

Mandible – MNCN-39918, right hemimandible with m1-m2.

Postcranial elements – MNCN-69984, distal epiphysis of right humerus.

Institutional abbreviations

ACA, Çalta identification acronym of the Musée National d'Histoire Naturelle (France); AMNH, American Museum Natural History, New York (USA); F:AM, Frick Collection, Department of Vertebrate Paleontology, American Museum of Natural History GNM, Georgian National Museum, Tbilisi (Georgia); HMNH, Hungarian Museum of Natural History, Budapest (Hungary); IGF, Museum of Natural History, Geological and Paleontological section, University of Florence (Italy); MNCN, Museo Nacional de Ciencias Naturales-CSIC, Madrid (Spain); MNHN, Musée National d'Histoire Naturelle, Paris (France); MZUF, Museum of Natural History, "La Specola" Zoology section, University of Florence (Italy); THP, Tianjin Museum (China).

Measurement abbreviations

Cranium: Ect, Ectorbitale-Ectorbitale (frontal width); ECW, splanchnocranium width measured at the external upper canine alveoli; FL, Prosthion-frontal midpoint (facial length); FMH, foramen magnum height; GNL, Nasion-Rhinion (greatest length of the nasals); GPW, greatest palatal width; LB, length of the tympanic bulla; LCM, length from the distal margin of the upper canine to the Basion; MOH, maxilla-orbit height (measured from the midpoint to M1 alveolus to the border to the orbit at that level); M2B, length from the distal margin of the M2 to the mesial border of the tympanic bulla; PwP1, Palatal width at P1; SCL, Prosthion-Nasion (splanchnocranium length).

Teeth: L, mesiodistal length; A C-M2 L, alveolar length of the upper teeth from the distal margin of the upper canine alveolus to the distal margin of the second molar; C-M2 L, length of the upper teeth from the upper canine to the second molar; M1–M2 L, upper molar row length; P1–M2 L, upper cheek tooth row length; P1–P4 L, upper premolar row length; trm1, trigonid of m1; tdm1, talonid of m1; W, buccolingual width.

Mandible: HR, mandibular corpus height distal to m1 alveolus; Mm1B, mandibular corpus breadth below themed point of the m1; Mp4H, mandibular corpus height distal to p4 alveolus;

Postcranials: Bd, breadth of the distal epiphysis; BG, breadth of the glenoid cavity of the scapula; Bp, breadth of the proximal epiphysis; BPC, greatest breadth across the coronoid process; DC, depth of the caput femoris; Dd, depth of the distal epiphysis; Dp, depth of the proximal epiphysis; DPA, depth across the processus anconaeus; GLP, greatest length of the processus articularis.

SYSTEMATIC PALEONTOLOGY

Order **Carnivora** Bowdich, 1821

Suborder **Caniformia** Kretzoi, 1943

Family **Canidae** Fischer, 1817

Subfamily **Caninae** Fischer, 1817

Tribe **Vulpini** Hemprich and Ehrenberg, 1832

Genus *Nyctereutes* Temminck, 1838

Nyctereutes donnezani (Depéret, 1890)

Synonyms: *Vulpes donnezani* Depéret, 1890

Type locality: Perpignan, France

Age: Early Pliocene, MN15

Differential diagnosis: Medium-sized *Nyctereutes*, smaller than *N. tingi* but similar in size to other Eurasian species, such as *N. sinensis*, and considerably larger compared to extant *N. procyonoides*.

Upper molars tend to be buccolingually narrow compared to *Vulpes* and also to *N. tingi*, but not mesiodistally elongated as in *N. procyonoides*, *N. sinensis*, *N. vulpinus* and *N. megamastoides*. In the mandible, the subangular lobe is generally more prominent than in *N. tingi*, but not to the extent of species like *N. procyonoides*, *N. sinensis*, *N. vulpinus* and *N. megamastoides*. The angular process is enlarged compared to the hook-shaped morphology observed in *N. tingi*, although *N. megamastoides* and the extant *N. procyonoides* have dorsoventrally larger angular processes. Lower premolars are more buccolingually compressed compared to other species. The m1 is reduced in width resembling that of *N. tingi*, with a talonid not enlarged unlike those of *N. sinensis* or *N. megamastoides*.

Description of Layna material

Cranium and cranial fragments – MNCN-63662 is a rather damaged and broken cranium, especially in the neurocranium portion (Fig. 2). In dorsal view, the cranium is considerably elongated, especially the splanchnocranium. The nasals are short, as they end before the maxillofrontal suture. In lateral view, the cranium profile is rather straight and the cranium appears short in height, although this morphology might be due at least in part to the dorsoventral diagenetic compression of the neurocranium. The orbit is large and with oval-like shape, in lateral view. The postorbital processes are broken. The specimen is considerably damaged at level of the postorbital constriction and it is difficult to estimate its actual width. This taking into account the state of preservation of the specimen and the morphology of the dorsal portion of the postorbital processes (which show a shallow depression, compatible with the vulpine crease), the frontal sinuses seem to be very poorly developed. The sagittal crest seems to be very low. In dorsal view, the braincase appears inflated, globular, but being broken and deformed, its original morphology is difficult to assess. The occipital region is badly damaged. The tympanic bullae are rather short mesiodistally, rounded in ventral view and considerably inflated. In ventral view, the palate is long and narrow, even at level of M1. It seems to end slightly caudally to the distal margin of M2.

Upper teeth – Incisors possess a large main cusp and two accessory small accessory cusps. The I3 is very similar in morphology to the other incisors. The C is considerably compressed buccolingually, with a high and pointed cusp. The premolars are separated by diastemata. The P1 has a conical, single cusp. The P2 has a large and high protocone and no distal accessory cusps. The P3 is similar to P2, but larger, with a distal cusp-like cingulum. The position of the P4 protocone is variable in the analyzed sample, although in the majority of the

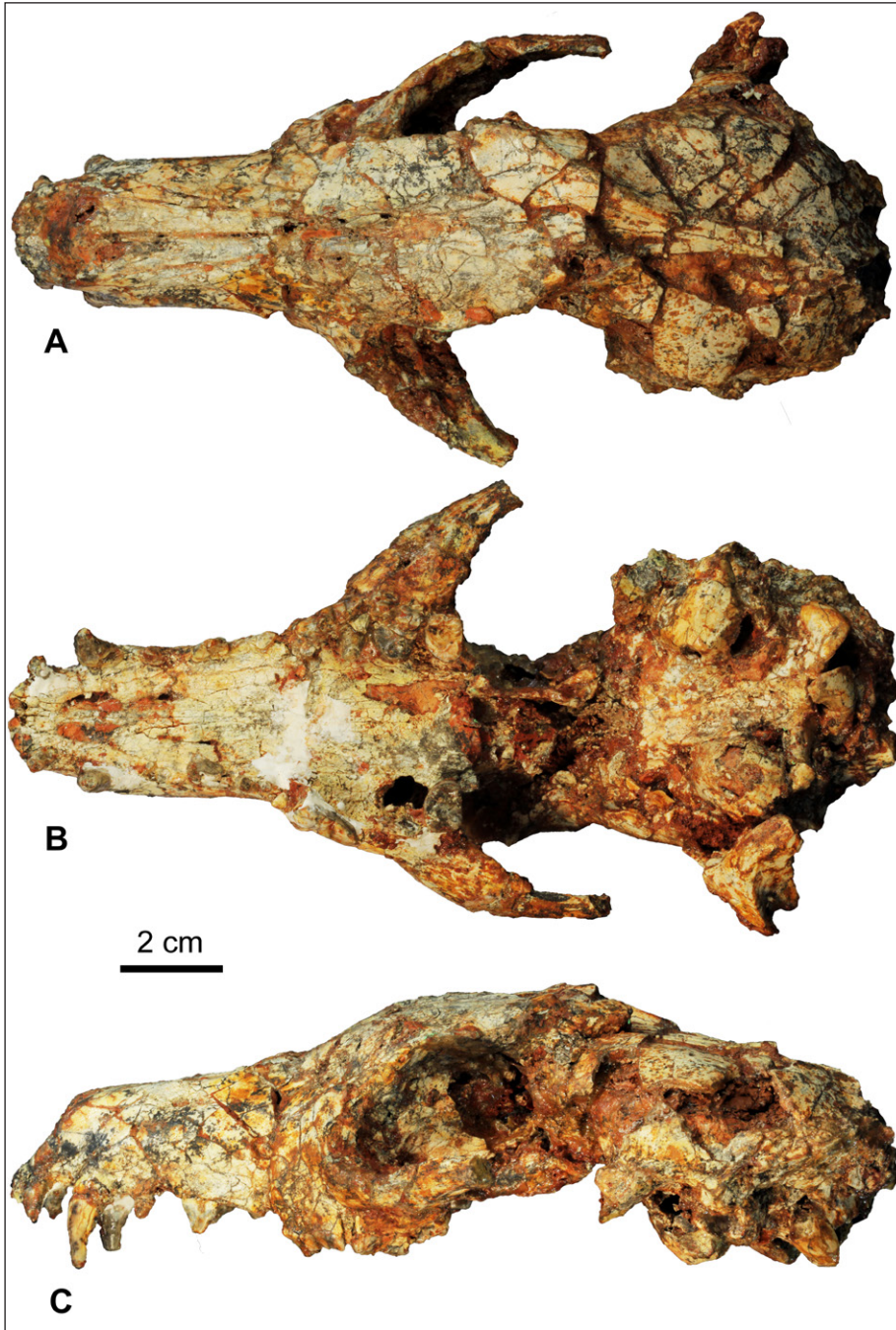


Fig. 2 - *Nyctereutes donmezani* from Layna, MN15 (Spain) – MNCN-63662, cranium in dorsal view (A), ventral view (B) and lateral view (C).

specimens, its exceeds mesially the mesial margin of the tooth (Fig. 3B-C; see MNCN-62481 in Fig. 3D as an example of different protocone mesial development). This cusp is large, high and pointed. On the opposite side of the protocone, there is a prominent and cusp-like mesial cingulum (almost in a parastyle). The P4 is overall compressed buccolingually, with a low but mesiodistally elongated paracone and a short metastylar blade. On the lingual side of the tooth, there is a continuous cingulum. The M1 is extends lingually with an elongated shape in occlusal view (Fig. 3E-F). The paracone is similar

in size compared to the metacone, although higher. The M1 protocone and metaconule are well-developed and there is a prominent protoconule. The hypocone is generally large-based and can be separated from the lingual cingulum by a small furrow. The cingulum is strong on the buccal and on the mesial sides. The M2 possesses a larger paracone compared to the metacone, a large protocone and smaller but visible protoconule and metaconule (Fig. 3F-G). The protocone and the metaconule are connected by the postprotocrista. Lingually, there is a cingulum-like hypocone.

Mandible – The corpus is rather low and slender (Fig. 4). Its ventral margin in lateral view, is slightly arched. In occlusal view, the lower tooth row appears straight. In buccal view, lower premolars do not show diastemata between them. The masseteric fossa is relatively deep and the ramus is rostrocaudally large, stout and rather elevated over the corpus. In the angular region, the subangular lobe is slightly developed, in lateral view, in with the shape of a short bulging of bone. The angular process is large and stout (Fig. 4I–J and L–M). MNCN-39917 (Fig. 4A–C) is the specimen in which the distal portion is better preserved but the angular process is broken.

Lower teeth – The incisors are small. The c is low-crowned. The lower premolars are mesiodistally short and possess very high protoconids (Fig. 4). Both p2 and p3 do not possess distal accessory cuspid. In occlusal view, the p4 is oval-shaped. It has a large accessory cuspid closely attached to the protoconid and a strong distal cingulid. The m1 paraconid is short, whereas the protoconid is high, not arched distally (Fig. 4). The metaconid is large and individualized from the protoconid, and it slightly projects on the lingual side. On the talonid, there is a large hypoconid and a smaller entoconid (with generally no difference in height between them) not connected by any cristid. Between the metaconid and entoconid, there is generally one large accessory cuspid. In almost all the specimens, a cristid bounds the distal margin of the m1 and connects the distal sides of the entoconid and the hypoconid (Fig. 4C, F, H, P). The m2 is generally bean-shaped in occlusal view, with a conspicuous mesiobuccal cingulid (Fig. 4). The protoconid and metaconid are large and equal in size. Mesially to these cuspids, there is generally a round cristid with a cuspid on it. On the talonid, there is a large hypoconid and, generally, one or more accessory cuspids behind the metaconid. The m3 is oval and possesses two equal-sized cuspids.

Postcranial elements – Scapulae. Among the various scapulae recovered from the site of Layna, only two fragments are in good state of preservation (i.e., MNCN-62577 and MNCN-62633) (Fig. 5). Nevertheless, these specimens preserve almost only the glenoid cavity and very little portion of the ala scapulae. The glenoid cavity outline is sub-rounded in shape. The supraglenoid tubercle is hooked with a stout coracoid process directly and closely attached to the medial margin of the tubercle.

Humerus. On the proximal epiphysis, there is

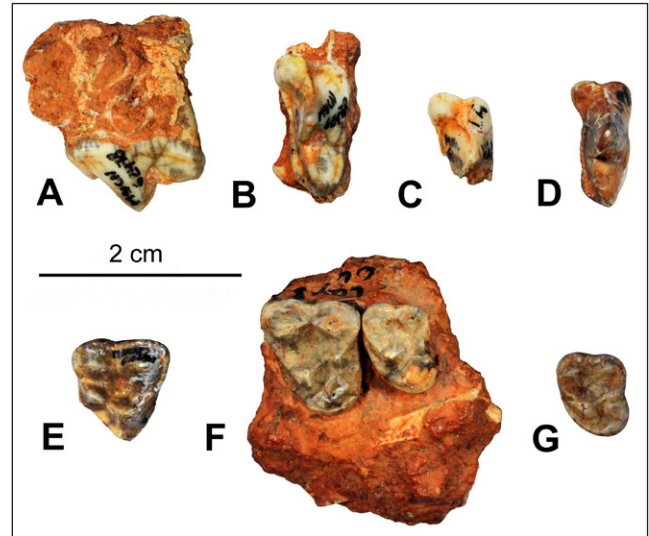


Fig. 3 - *Nyctereutes donmezani* from Layna, MN15 (Spain) – MNCN-62478, left maxillary fragment with P4, in buccal (A) and occlusal view (B). MNCN-62479, left P4, in occlusal view (C). MNCN-62481, left P4, in occlusal view (D). MNCN-62492, left M1, in occlusal view (E). MNCN-39920, left maxillary fragment with M1–M2, in occlusal view (F). MNCN-62493, left M2, in occlusal view (G).

a robust head. The greater tubercle is slightly higher compared to the head, and it is considerably enlarged (Fig. 5). The lesser tubercle is quite prominent and large, in palmar view. On the distal epiphysis, there is a round supratrochlear foramen. In cranial view, the distal articular surfaces appear compressed dorsoventrally in comparison to its width, especially the capitulum, although the medial side of the trochlea extends distally (Fig. 5). Furthermore, the lateral side of the distal articular surface is inclined compared to the medial side and the vertical axis of the diaphysis. The distal epicondyles are both well-developed, although the medial is larger than the lateral. In medial view, MNCN-62502 shows a prominent supratrochlear crest (Fig. 5).

Radius. In proximal view, the proximal articular area is bean-shaped. The coronoid process is a prominent tip, in cranial view. On the cranial side of the distal portion, there is a swelling of bone, particularly prominent in MNCN-70905 (Fig. 5G), identified by the wide grooves of the extensor carpi radialis and extensor digitalis communis muscles.

Ulna. The tuberosity of the olecranon is knob-like in shape. On the medial side, there is a deep fossa below this tuberosity. The lateral coronoid process is greatly reduced compared to the medial one, resembling more a small bone prominence. The medial coronoid process is rather thin

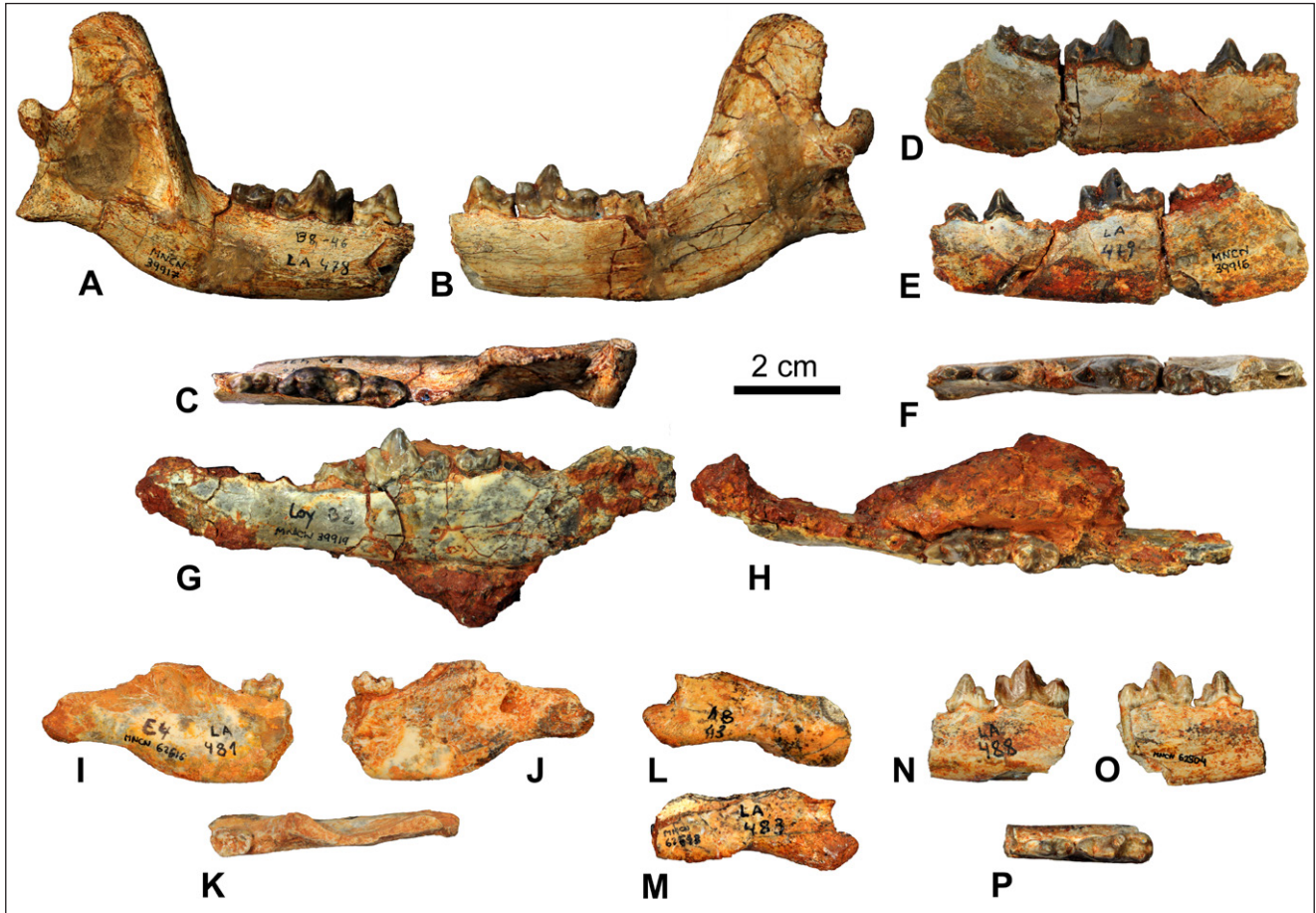


Fig. 4 - *Nyctereutes donnezani* from Layna, MN15 (Spain) – MNCN-39917, right hemimandible fragment with p4-m2, in buccal view (A), lingual view (B), occlusal view (C). MNCN-39916, right hemimandible fragment with p2-p3 and m1-m3, in buccal view (D), lingual view (E), occlusal view (F). MNCN-39919, right hemimandible fragment with p4-m2, in lingual view (G), occlusal view (H). MNCN-62616, right hemimandible fragment with m2, in buccal view (I), lingual view (J), occlusal view (K). MNCN-62618, right hemimandible fragment, in buccal view (L), lingual view (M). MNCN-62504, left hemimandible fragment with p4-m1, in buccal view (N), lingual view (O), occlusal view (P).

and compressed mediolaterally instead of expanding medially, it projects cranially, if observed in proximal view (Fig. 5I).

Femur. MNCN-52972 is an almost complete femur, missing only the greater trochanter (Fig. 5J). It is rather shortened, with thick diaphysis and mediolaterally large epiphyses. In medial view, the lesser trochanter is large and prominent. On the diaphysis, there are no relevant grooves visible. On the cranial side of the distal epiphysis, the ridges of the distal articulation are prominent. In plantar and distal views, the intercondylar space is large. Dorsal to the lateral condyle, in plantar view, there is a prominent supracondylar tuberosity.

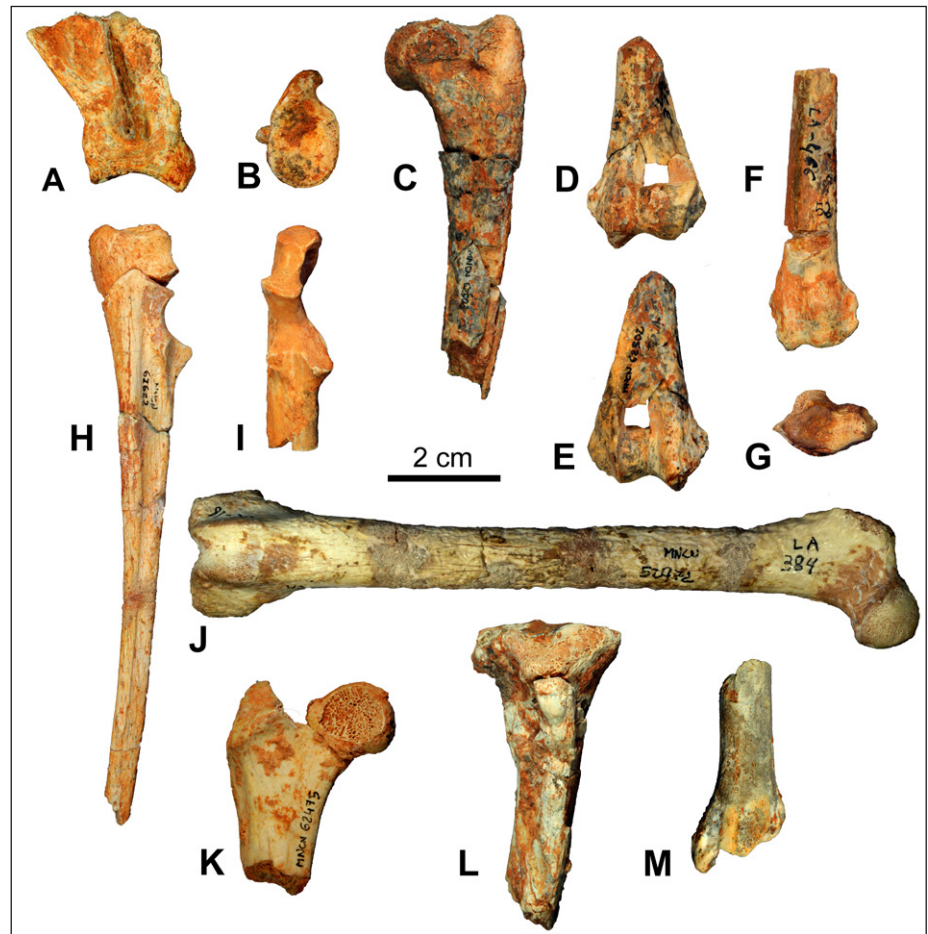
Tibia. In cranial view, the diaphysis of the tibia seems markedly curved, especially near the proximal epiphysis (Fig. 5L). Distally, the medial malleolus is rather enlarged and extended distally (Fig. 5M).

Comparison

Although damaged, MNCN-63662 is one of the most complete crania of *N. donnezani* reported in the literature (Fig. 2). MNCN-63662 shows numerous similarities with the cranium of *N. tingi* (e.g., F:AM 96575; THP 22714). For instance, both species are large-sized, possess diastemata between upper premolars, and the splanchnocranium is rather elongated compared to the neurocranium. Besides the larger overall size, the crania of *N. sinensis* from Yushe Basin, *N. vulpinus* from St. Vallier or *N. megamastoides* of Europe show a smaller basicranial area compared to that of *N. donnezani* and similar proportions between the neurocranium and the splanchnocranium. Other features cannot be discussed due to the state of preservation of the fossil from Layna.

The set of morphologies of the Layna material is consistently primitive if compared to the

Fig. 5 - *Nyctereutes donnezani* from Layna, MN15 (Spain) – MNCN-62577, fragment of right scapula, in lateral view (A) and distal view (B). MNCN-62503, fragment of left humerus, in lateral view (C). MNCN-62502, fragment of left humerus, in dorsal view (D) and palmar view (E). MNCN-13654, fragment of left radius, in dorsal view (F). MNCN-70905, fragment of left radius, in distal view (G). MNCN-62622/549, right ulna, in lateral view (H). MNCN-62623, fragment of right ulna, in dorsal view (I). MNCN-52972, right femur, in dorsal view (J). MNCN-62473/75, proximal epiphysis of right femur, in dorsal view (K). MNCN-62488, proximal epiphysis of left tibia, in dorsal view (L). MNCN-62485, distal epiphysis of right tibia, in dorsal view (M).



features characterizing *N. sinensis*, *N. vulpinus* and *N. megamastoides*. For instance, the latter species show a high angle between the mandibular corpus and ramus, in the area of the subangular lobe; additionally, the development of the angular process or sub-quadrangle morphology of M1 and M2 in *N. vulpinus*, *N. sinensis* and particularly *N. megamastoides* cannot be seen in *N. donnezani*. Similarly, *N. procyonoides* exhibits several features that are also highly derived and not comparable to those of *Nyctereutes* from Layna, e.g., the presence of a stronger parastyle on P4, the general morphology of the upper molars, the reduced development of the metacone and metaconule in the M1, the proportionally reduced metaconid on the m1, etc. The dentognathic features of *N. vulpinus* from St. Vallier are rather derived in comparison to those of the considered sample. For example, *N. vulpinus* possesses the M1 paracone slightly larger than the metacone; a quadrangle occlusal shape of the M2; a well-developed subangular lobe, stronger than that of *N. donnezani*. Other features that distinguish *N. vulpinus* from the specimens from Layna are the thin and sharp angular process and the relative development of the

pterygoideus medialis muscle scars on the medial side of this process (Fig. 6). Although the characters of the taxon from St. Vallier are more derived than those of *N. donnezani* from Perpignan and *Nyctereutes* from Layna, they are suggestive of a less advanced degree of adaptation to an hypocarnivorous diet similar to that of *N. sinensis* and in contrast to *N. megamastoides*.

The taxa showing primitive morphologies close to those observed in the Layna sample are *N. tingi* from numerous localities of the Yushe Basin (China) and *N. donnezani* from La Gloria 4 (Spain) and Perpignan (France). Among the shared features, the poorly developed subangular lobe, the morphology of the upper molars, and their reduced width can be pointed out.

Regarding the postcranial sample, the humeri from Layna (e.g., MNCN-62503) possess a robust head that extends palmarly, with an oval shape when observed in proximal view. Conversely, in the humerus of *N. megamastoides* from Perrier-Les Etouaires or of the extant *N. procyonoides*, the caput humeri is rather round in shape in proximal view. The greater tubercle of the Layna sample resembles

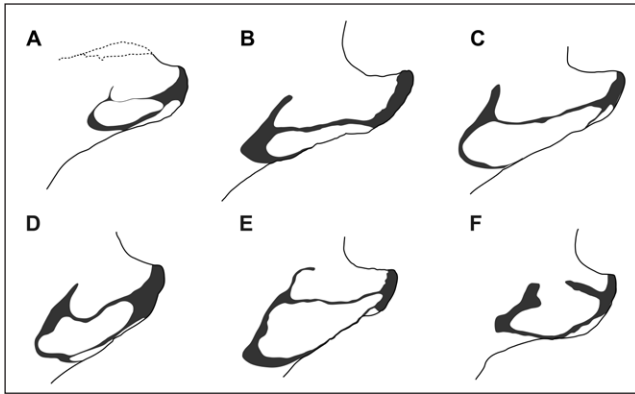


Fig. 6 - Comparative schematic representation of the rami of the medial pterygoideus muscle on the medial side of the angular process in different *Nyctereutes* species: A) *N. donnezani* from Layna; B) *N. tingi* from the Yushe Basin; C) *N. vulpinus* from St. Vallier; D) *N. megamastoides* from Senéze; E) *N. sinensis* from the Yushe Basin; F) extant *N. procyonoides*. Muscle insertions are represented by scars or rough surfaces on the angular process. All outlines were rescaled to appear of the same dimensions.

that of *N. procyonoides*, whereas it is proportionally larger than that of *N. megamastoides*. Compared to these two species, the intertubercular sulcus of the specimens from Layna (e.g., MNCN-62503 and MNCN-69984) is reduced and narrow if compared to the condition of *N. megamastoides* and *N. procyonoides*. Moreover, the lesser tubercle appears reduced compared to that of both the extant *N. procyonoides* and *N. megamastoides*. In the distal epiphysis of the humerus, the majority of the specimens from Layna possesses a large, proximodistally high capitulum, similar to that of *N. donnezani* of Perpignan and unlike *N. megamastoides* of Perrier-Les Etouaires, *N. vulpinus* from St. Vallier and extant *N. procyonoides*. In distal view, the incision for the articulation of the olecranon of the ulna is proportionally narrower compared to that of *N. megamastoides* and *N. procyonoides*. In the same view, the distal epiphysis appears stout and craniopalmarly enlarged compared to *N. procyonoides*, *N. donnezani* from Perpignan and *N. megamastoides* from Perrier-Les Etouaires. In cranial view, the trochlea of *N. procyonoides* tends to be strongly inclined medially. In the fossil species, this feature is not clearly marked. The features of the distal portion of the radius resemble those of *N. donnezani* from Perpignan for the elongation in lateral direction of the distal articular surface (in distal view), correspondingly to a compression in craniopalmar direction. This rectangular shape contrasts with the condition seen in *N. megamastoides*. Moreover, another common feature between the

specimens from Layna and Perpignan, is the bone swelling on the cranial side of the distal epiphysis, which is conversely smaller in *N. megamastoides*. Both *N. donnezani* from Perpignan and the specimens of Layna possess a well-developed and large groove for the muscle extensor radialis carpi whereas the of the muscles extensor digitorum communis and extensor obliquus carpi are reduced.

The ulna of *N. megamastoides* shows an enlarged, prominent and shelf-like medial coronoid process, different from that of *N. procyonoides* and especially from that of the sample from Layna and *N. donnezani* from Perpignan. In these two latter taxa, the medial coronoid process although larger than the lateral one, is thinner and receding compared to that of *N. megamastoides*.

The neck of the femur of the specimens of Layna (e.g., MNCN-62473/75 or MNCN-52977), is stout as in *N. donnezani*, while it is more slender in *N. megamastoides* and *N. procyonoides*. The lesser trochanter is prominent in lateral view and well developed compared to *N. megamastoides* from Perrier and especially to the extant *N. procyonoides*. The third trochanter is peculiarly larger in the sample of Layna than in *N. procyonoides*.

A relevant difference between the tibiae of Layna and other Eurasian samples lie in the morphology of the distal articular surface: the plantar margin of the surface is reduced in lateral length compared to the cranial margin, giving a triangular shape to the tibial trochlea in distal view. This feature resembles that of *N. donnezani* from Perpignan but contrast with *N. megamastoides* and *N. procyonoides*.

All measurements of the *Nyctereutes* sample from Layna are shown in Tables 1-7.

Log-ratio diagrams (Fig. 7) were used to test the affinities of the Layna sample in comparison to the variability of the Eurasian fossil taxa. These diagrams were used to compare the mean dental measures of Eurasian Pliocene-Pleistocene species and of the extant *N. procyonoides*, which was used as a standard reference in all the diagrams. The graph of Fig. 7A highlights the similarity in tooth proportions between the Layna material and *N. donnezani* from Perpignan. Therefore, these morphometric results reinforce those obtained from the morphological comparison and support the attribution of the Layna sample to *N. donnezani*. In general dental proportions, the sample from Layna is significantly larger than the extant *N. procyonoides* but similar in size to

Catalog. N°	FL	SCL	GNL	Ect	ECW	GPW	MOH	PwPI	LB	M2B	FMH	LCM
MNCN63662	82.7	61.8	44.4	35.7	27	44	16.1	18.5	16	35.5	11.8	126.9

Tab. 1 - Cranial measurements (mm) of *Nyctereutes danzevskii* from Layna. For measurement abbreviations, see the main text.

Catalog. N°	side	C L	C W	P1 L	P1 W	P2 L	P2 W	P3 L	P3 W	P4 L	P4 Lmax	P4 W	M1 L	M1 W	M2 L	M2 W	C-M2 L	A C-M2 L	P1-M2 L	P1-P4L	M1-M2 L	
MNCN39920	L	-	-	-	-	-	-	-	-	-	-	-	9.7	11.2	6.4	8.3	-	-	-	-	-	15.8
MNCN39921	L	-	-	-	-	-	-	-	-	12.1	13.1	6.2	10.6	11.9	-	-	-	-	-	-	-	-
MNCN63662	L	7.2	4.6	3.8	2.5	7.8	2.8	-	-	13.3	15.1	-	10.7	11.2	7.1	9	70.3	62.2	58.1	41.3	18	

Tab. 2 - Measurements (mm) of associated upper teeth of *Nyctereutes danzevskii* from Layna. For measurement abbreviations, see the main text.

Catalog. N°	side	L	W	Lmax
MNCN62494	C	L	6.4	4.3
MNCN62482	P2	R	6.5	2.9
MNCN62478	P4	L	12.8	7.4
MNCN62479	P4	L	-	6.1
MNCN62481	P4	L	12.8	7
MNCN62491	M1	R	9.7	-
MNCN62492	M1	L	9.95	10.5
MNCN62493	M2	L	6.8	8.1

Tab. 3 - Measurements (mm) of isolated upper teeth of *Nyctereutes danzevskii* from Layna. For measurement abbreviations, see the main text.

Catalog. N°	Side	p2 L	p2 W	p3 L	p3 W	p4 L	p4 W	m1 L	m1 W	trml L	tdml W	m2 L	m2 W	m3 L	m3 W	Mp4H	MmlH	MmlB	HR
MNCN39916	R	6.1	2.5	7.5	2.7	-	-	15.6	5.9	10	5.8	7.8	5.4	4.1	3.6	-	-	-	-
MNCN39917	R	-	-	-	-	9.1	3.9	14.8	6.2	9.2	6.1	8	-	-	13.9	15.9	7.8	41	
MNCN39918	R	-	-	-	-	-	-	15.1	6.4	9.8	6.3	8.9	6.3	-	-	-	-	-	-
MNCN39919	R	-	-	-	-	9.1	-	15.7	-	10	-	8.4	6.7	-	-	17	-	-	-
MNCN62504	L	-	-	-	-	9	3.5	13.6	5.2	8.4	5.1	-	-	-	-	14	-	-	-

Tab. 4 - Measurements (mm) of mandibles and associated lower teeth of *Nyctereutes danzevskii* from Layna. For measurement abbreviations, see the main text.

Catalog. N°	Side	L	W	trml L	tdml W
MNCN62495	c	R	6.8	4.3	-
MNCN62497	c	R	6.8	4.3	-
MNCN62651	c	R	6.7	4.5	-
MNCN70008	c	L	6.6	4.49	-
MNCN70009	c	R	6.1	4.4	-
MNCN62621	p1	R	3.5	2.1	-
MNCN71085	p3?	R	7.1	3	-
MNCN62519	m1	R	17	6.3	11
MNCN62608	m1	L	6.7	-	6.3
MNCN62609	m1	R	6.8	-	-
MNCN71087	m1	R	16	6.7	11.7
MNCN62616	m2	R	7.6	5.2	-
MNCN62619	m2	L	8.6	5.7	-
MNCN70007	m3	L	4	3.7	-

Tab. 5 - Measurements (mm) of isolated lower teeth of *Nyctereutes danzevskii* from Layna. For measurement abbreviations, see the main text.

	Scapula		Humerus		Radius				Ulna	
	GLP	BG	Dp	Bd	Bp	Dp	Bd	Dd	DPA	BPC
Min	18,5	10,1	25,5	20,4	12,0	7,7	15,1	8,6	16,7	7,0
Max	21,6	13,1	29,3	25,5	13,2	8,5	17,0	10,3	18,4	11,0
Mean	19,4	11,5	27,4	22,9	12,4	8,2	16,0	9,6	17,4	9,1
Stand. De	1,3	1,0	2,7	2,1	0,7	0,4	1,0	0,7	0,9	1,3
N° elem	5	7	2	4	3	3	4	4	3	6

Tab. 6 - Measurements (mm) of the forelimb bones of *Nyctereutes donnezani* from Layna. For measurement abbreviations, see the main text.

	Femur				Tibia		
	Bp	DC	Bd	Dd	Bp	Bd	Dd
Min	28,4	12,0	21,4	18,8	24,3	15,3	11,4
Max	29,0	13,1	23,8	24,7	26,2	16,0	11,8
Mean	28,7	12,5	22,5	20,9	25,5	15,7	11,6
Stand. De	0,4	0,5	0,9	2,8	1,0	0,5	0,3
N° elem	2	4	5	5	3	2	2

Tab. 7 - Measurements (mm) of hindlimb bones of *Nyctereutes donnezani* from Layna. For measurement abbreviations, see the main text.

the fossil species of *Nyctereutes*, as shown in Fig. 7A. When considered all together, the proportions and size the Perpignan, La Gloria 4 plus Layna samples (*N. donnezani* from Western Europe of Fig. 7B) fall between those of *N. procyonoides* and *N. tingi*, being the former considerably smaller and the latter substantially larger than the other taxa. Remarkable is the similarity between the pattern of dental proportions of *N. donnezani*, *N. sinensis* and especially *N. vulpinus*, besides the presence of some derived morphological features in the two latter (e.g., equal-sized paracone and metacone on M1; quadrate occlusal shape of M2) (Fig. 7B). The general dental proportions and size of *N. megamastoides* do not differ significantly from *N. sinensis* and *N. vulpinus*, except for the proportionally longer M2, the enlarged m1 and the wider m2.

Nyctereutes cf. *megamastoides* (Pomel, 1842)

Synonyms: *Canis megamastoides* Pomel, 1842.

Type locality: Perrier-Les Etouaires, France.

Age: Late Pliocene, MN16.

Differential diagnosis: The cranium tends to be shortened rostrocaudally. The upper molars tend to have squared outline in occlusal view, unlike the buccolingually wider shape of *N. donnezani* and *N. tingi*. In M1 and M2, the paracone and metacone are equal in size like in *N. donnezani* but in contrast to *N. sinensis* and *N. vulpinus*. *Nyctereutes megamastoides* possesses a mandible with a greatly developed subangular lobe similar and even more prominent compared to *N. sinensis* and *N. vulpinus*. The angular process in *N. megamastoides* is enlarged in dorsoventral direction, with large insertion areas for branches of the pterygoid muscle (particularly the superior one). The m1 trigonid tends to be shortened compared to primitive taxa of the genus and the talonid is buccolingually enlarged. The m1 metaconid

is enlarged and extends lingually. The cuspids of the m1 talonid are generally joined by a marked cristid unlike other species of *Nyctereutes*. The m2 is rather enlarged in its mesial portion, with a larger protoconid compared to the metaconid. Accessory cuspids are present in the distal portion of the m2.

Other localities: Senéze, Pardines (France); Villarroya (Spain); San Giusto, Montopoli, Collepardo (Italy); Dafnero, Volax, Sesklon, Vatera-F (Greece); Kvabebi (Georgia); Volovaya Balka (Russia).

Description of Layna material

Upper teeth – The maxillary fragment MNCN-39921 preserves complete P4 and M1. The P4 (L= 12.1 mm; Lmax= 13.1 mm; W= 6.2 mm) has a large protocone that lies at the same level of the mesial margin of the P4 or slightly advanced (Fig. 8A-B). Lingually there is a strong cingulum whereas on the mesial side there is a faint one. The paracone is high and pointed and the metastylar blade is short. The M1 (L= 10.6 mm; W= 11.9 mm) is quadrangular in occlusal view (Fig. 8A-B). The paracone is equal in size as the metacone, but slightly higher. The M1 protocone is large and the metaconule is reduced; the protoconule is evident. On the mesial side, there is an expanded and prominent cusp-like cingulum. The hypocone is large. The buccal cingulum is prominent.

Lower teeth – The m1 dimensions of MNCN-39918 are: L= 15.1 mm; W= 6.4 mm; tr L= 9.8 mm. The m1 protoconid is markedly higher than the low paraconid (Fig. 8C-E), which is slender in occlusal view. The metaconid is prominently large and separated from the protoconid. Together with the talonid, it extends lingually. The hypoconid is larger and

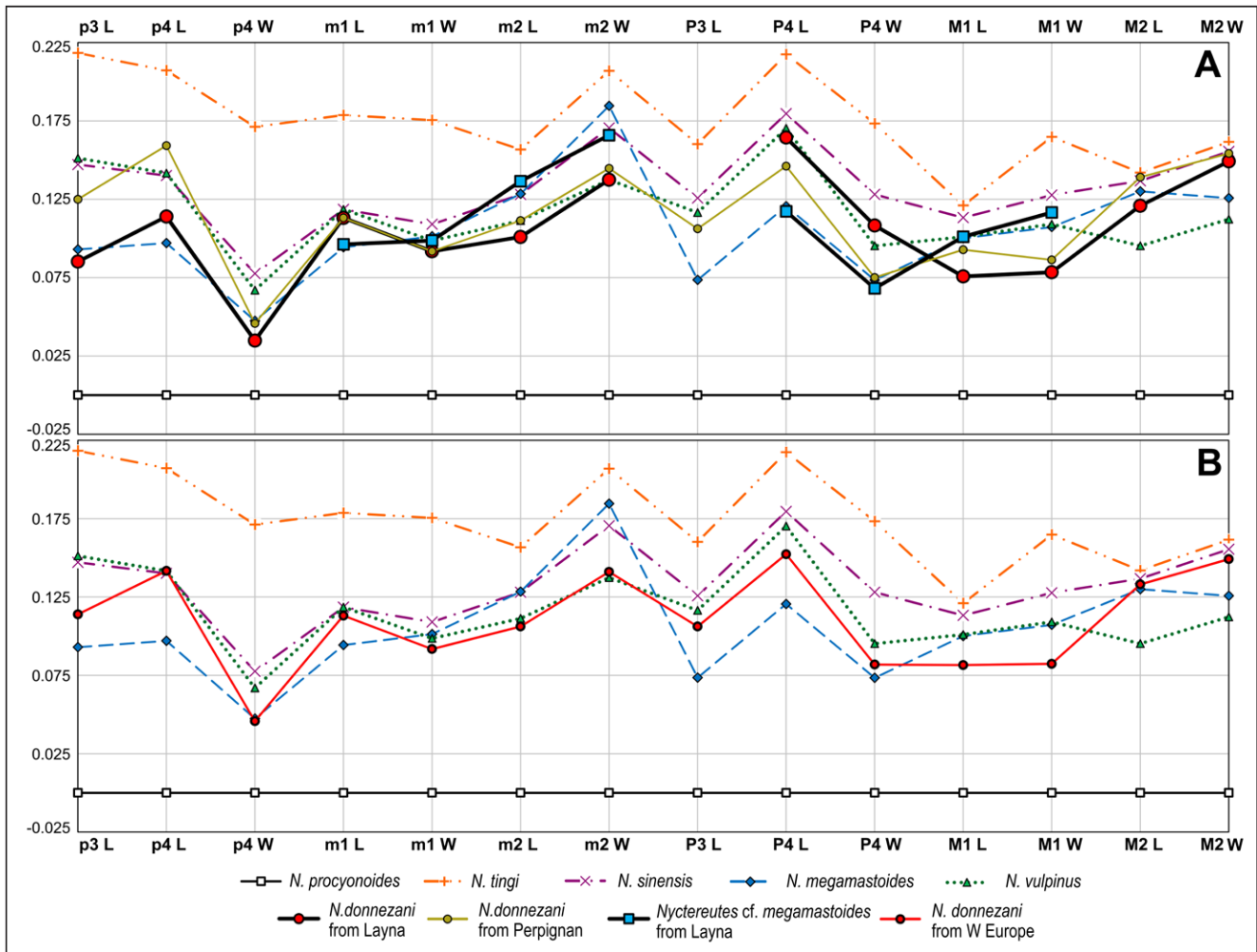


Fig. 7 - Log-ratio diagrams on selected upper and lower tooth variables in Plio-Pleistocene species and selected samples of *Nyctereutes* as compared to the extant *N. procyonoides*. A) Log-ratio diagram on the different samples of Layna (*N. donnezani* and *N. cf. megamastoides*) in comparison to the Plio-Pleistocene species (*N. sinensis*, *N. tingi*, *N. vulpinus*, *N. megamastoides* and the type sample of *N. donnezani* from Perpignan) and *N. procyonoides*. B) Resumming log-ratio diagram showing the pattern of dental proportions in the fossil Eurasian species as compared to the extant *N. procyonoides* (used as the reference baseline). Here the proportions of *N. donnezani* are the resulting from the combination of the sample of La Gloria 4, Perpignan and Layna. The extant *N. procyonoides* is used as the reference baseline in both diagrams.

higher compared to the entoconid; a short cristid connects them, prominent, especially on the entoconid. Between the metaconid and the entoconid there are two large accessory cusplids. In occlusal view, the m2 (L= 8.9 mm; W= 6.3 mm) is bean-shaped with a conspicuous buccal development of the cingulid, especially mesially (Fig. 8E). The protoconid is similar in size to the metaconid. A cristid develops from the mesial side of the protoconid. On the talonid, there is the hypoconid and three prominent accessory cusplids behind the metaconid.

Postcranial elements – Humerus. It preserves only the distal portion (Bd= 29.3 mm). In cranial view, the distal articular surface of MNCN-69984 appears

elongated laterally especially in the capitulum (Fig. 8F). The trochlea, although damaged, is very high in proximodistal direction. The lateral side of the distal articular surface is strongly inclined laterally compared to the medial side, which is parallel to the vertical axis of the diaphysis. The epicondyles are well-developed and similar in size, both extended laterally. The olecranon fossa seems deep and large.

Comparisons

The position and the development of the P4 protocone is unusual compared to the rest of the sample from Layna: it is relatively reduced and close the paracone instead of having a strong and advanced mesial margin (Figs 3 and 8). The squared

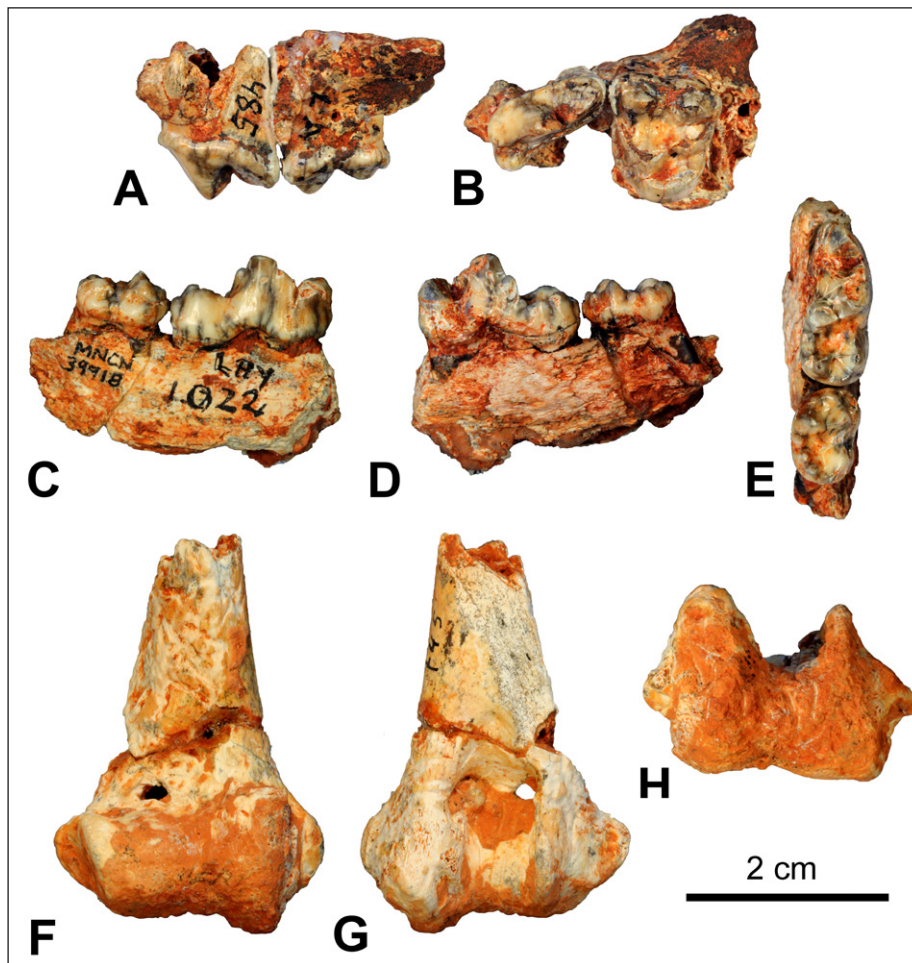


Fig. 8 - *Nyctereutes* cf. *megamastoides* from Layna, MN15 (Spain) – MNCN-39921, left maxillary fragment with P4-M1, in lateral view (A) and occlusal view (B). MNCN-39918, right hemimandible fragment with m1-m2, in buccal view (C), lingual view (D) and occlusal view (E). MNCN-69984, fragment distal epiphysis of right humerus, in cranial view (F), palmar view (G) and in distal view (H).

morphology of the upper molar of MNCN-39921 differs greatly from the other molars recovered from Layna. Particularly, the development of the mesial cingulum, with its short but prominent cusps, and the lingual shortening of M1 resemble the features observed in the specimens from Perrier-Les Etouaires, Dafnero, or Kvabebi and strongly contrast with those of *N. donnezani* from Layna or Perpignan and those of *N. tingi* from the Yushe Basin. For instance, no specimens of the analyzed sample of these two latter species show a buccolingual reduction of the M1, or possess the cusp-like cingulum. Even the more derived taxa, *N. sinensis* and *N. vulpinus*, do not possess a markedly enlarged and cusp-like cingulum on the mesial side of M1. The morphological analysis of the samples of *N. sinensis* and of *N. vulpinus* reveal that only the 14% and the 22% of the specimens, respectively, possessed large and cusp-like mesial cingulum. On the contrary, *N. megamastoides* and *N. procyonoides* almost always possess this morphology of the mesial cingulum of the M1 (95% and 90% of the considered sample). The morphology of the m1 is peculiar for the con-

spicuous enlargement of the metaconid and talonid, especially in occlusal view. The widening of the talonid area of the m1 compared to the trigonid is marked in the derived species *N. megamastoides* whereas in *N. donnezani* or even *N. sinensis* and *N. vulpinus*, this feature is not prominent. The presence of large accessory cusps on the lingual side of m1 and m2 and the cristid connecting the m1 hypoconid and the entoconid are further features that resemble *N. megamastoides* or *N. vulpinus* as *N. donnezani* does not possess the crista transversa. *N. sinensis* rarely possess accessory cuspid/cuspulids or this cristid between hypoconid and entoconid. Particularly, among the specimens of *N. sinensis* from Yushe Basin and Nihewan Basin only the 5% possessed a crista transversa. On the contrary, in *N. vulpinus* from St. Vallier the percentage of specimens with the cristid is above the 54%, but in the samples attributed to *N. megamastoides* (e.g., Perrier-Les Etouaires, Senéze, Kvabebi), the 90% of the specimens with preserved m1 show a prominent cristid between the m1 hypoconid and entoconid. In the extant *N. procyonoides*, the 72% of

the sample displayed a prominent crista transversa. The enlargement of the m1 talonid in buccolingual sense, visible in occlusal view, and the supranumerary cusplids on the lower molars contrast with the diagnostic features of *N. vulpinus* as described by Soria & Aguirre (1976) (viz. the elongated m1 and a reduced m2).

The humerus MNCN-69984 possesses features contrasting with *N. donnezani* from Perpignan and even other specimens from Layna. It resembles those of the material recovered from Perrier-Les Etouaires and attributed to *N. megamastoides*. For instance, in cranial view, the distal articular surface of MNCN-69984 shows an enlarged trochlea, greatly expanded compared to the short capitulum, similar to *N. megamastoides* from Perrier-Les Etouaires and from Kvabebi and the extant *N. procyonoides*. On the contrary, in *N. donnezani* from Perpignan and Layna, the trochlea and capitulum are similar in height. In lateral view, the distal epiphysis of the humerus of *N. megamastoides* is craniopalmarly more compressed compared to that of *N. donnezani*. The same difference is visible in *N. procyonoides* and *N. donnezani*.

The log-ratio diagram in Fig. 7A compares the proportions of the dental sample from Layna tentatively attributed to *N. cf. megamastoides* with those of Eurasian samples. Although fragmentary, the pattern of the Layna material in the graph clearly follows that of *N. megamastoides*, thus supporting the taxonomic attribution made on morphological ground.

DISCUSSIONS AND CONCLUSIONS

The origin of the genus *Nyctereutes* is still debated and rather dubious. Its earliest occurrence is represented by the species *N. tingi* from the Early Pliocene (correlable to MN14) localities of the Yushe Basin (Tedford & Qiu 1991). Nevertheless, the ancestor of this primitive Asian form is yet unknown. Another issue is the confusion regarding the relationship between *Nyctereutes* and other canids. Tedford et al. (1995, 2009) suggested a close phylogenetic affinity between *Nyctereutes* and *Cerdocyon* Smith, 1839 because of the retention of shared features like the presence of a developed subangular lobe, the expansion of the angular process, the development of the pterygoideus medialis scars on the lingual side of the angular process and

low-crowned canines. For this reason, they ascribed these two genera to the same subtribe *Cerdocyonina* within the tribe *Canini*, and therefore deeming a closer affinity to *Canis* Linnaeus, 1758 than to *Vulpes* Frisch, 1775. On the contrary, several genetic analyses (Wayne et al. 1997; Wayne & Ostrander 2007) grouped *Nyctereutes* within the tribe *Vulpini*, separated from the South American clade of *Canini* (which includes *Cerdocyon*). In our opinion, the ancestor of raccoon-dog-like canids is a member of *Vulpini* that spread into Eurasia from North America (center of origin of the tribe *Vulpini*, see Tedford et al. 2009) at the end of the Miocene and the morphologies shared by *Cerdocyon* and *Nyctereutes* are homoplasies resulting from convergent evolution to ecological adaptations.

After the appearance of *N. tingi*, the first record of a derived form, *N. sinensis*, is reported from Early Pliocene Chinese sites of the Yushe Basin (correlable to MN15). More or less contemporaneously, in Western Europe *N. donnezani* appears in the fossil record, first in Perpignan and subsequently in Layna. The features described above confirm the rather primitive state of this taxon, comparable to that of *N. tingi*. Nevertheless, Tedford & Qiu (1991), in their description of *N. tingi*, pointed out some differences between the Chinese taxon and *N. donnezani*. Among these, there is the larger size, the presence of incipient cristids connecting the hypoconid and the entoconid on m1, and the larger metaconule compared to the protoconule on M1. Other features used by the authors, e.g., the similar size of paracone and metacone in the upper molars and the similar morphology of the angular process, need to be reconsidered since in *N. donnezani* the buccal cusps have different size (Fig. 3) and the angular process, in medial view, has different morphology (Fig. 6). In fact, in *N. tingi*, the angular process is rather thin and has the shape of an elongated hook, whereas in *N. donnezani* it is enlarged and, to some extent, is morphologically closer to that of *N. sinensis* and *N. megamastoides*. Another difference between the Chinese and European taxa is that the record of *N. tingi* in the Yushe Basin seems to be uninterrupted from the earliest Pliocene to ca. 3 Ma, whereas *N. donnezani* has been described from few and sparse localities in Spain and France, referable to MN14 and MN15. These localities are La Gloria 4 (4.19 Ma; Domingo et al. 2013), Perpignan (Serrat-d'en-Vacquer, ca. 4 Ma; Clauzon et al.

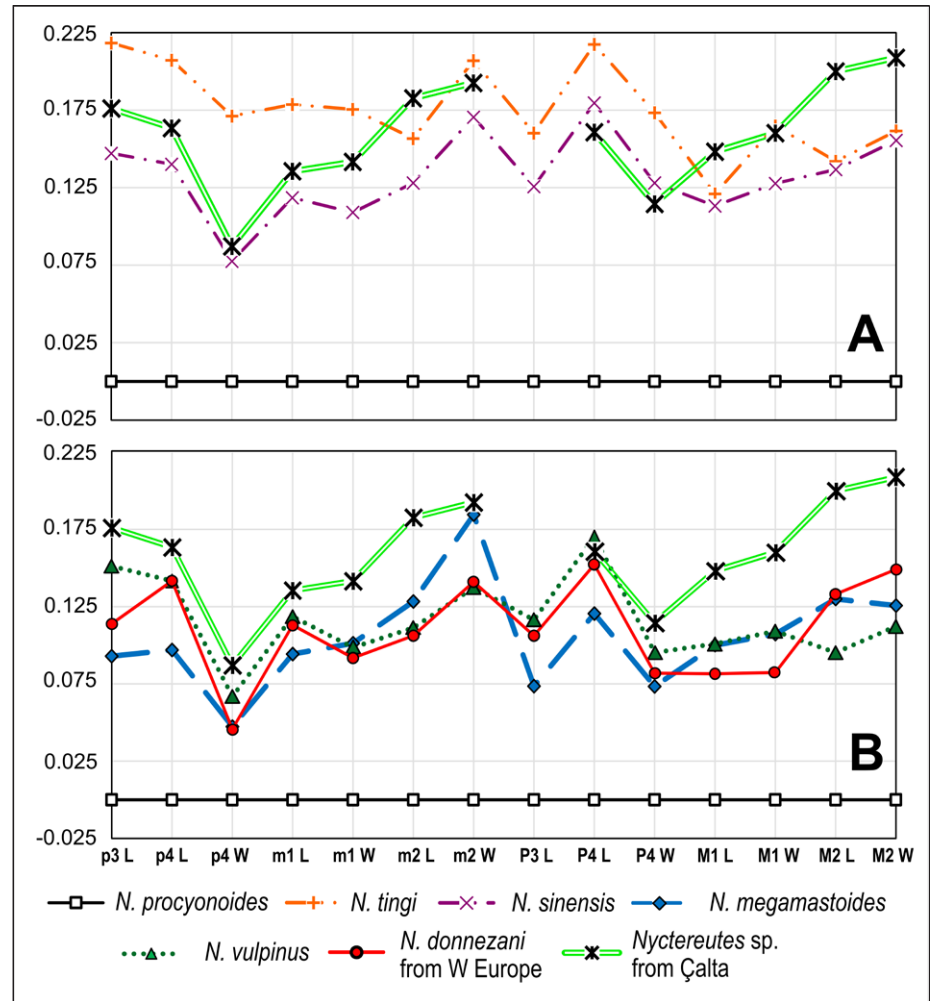
2015) and Layna (3.91 Ma; Domingo et al. 2013). A coeval record of the genus comes from the Turkish site of Çalta (Ankara Province, North-Western Turkey), correlated to some MN15 European localities (see among others Bernor & Sen 2017). The remains of *Nyctereutes* from Çalta, which include two well-preserved crania (MNHN.F.ACA291 and MNHN.F.ACA292 and some mandibular specimens (e.g., MNHN.F.ACA549 and MNHN.F.ACA294), were attributed to *N. donnezani* by Ginsburg (1998). Several cranial and dentognathic features support this attribution, e.g., the rostrocaudal elongation of the cranium in dorsal view (although the crania suffered of a certain degree of lateral diagenetic compression, considering the morphology of the nasal area in dorsal view; this compression might result in an overall impression of a prominent rostrocaudal elongation); and the morphology of the subangular region, with no or poorly developed subangular lobe. Other characteristics, on the contrary, differ from the type material of Perpignan and from that of Layna. Unlike *N. tingi*, *N. sinensis* and *N. vulpinus*, the absence or the great reduction of the frontal sinus, the reduced length of the area caudal to the postorbital processes and the marked postorbital constriction are features similar to the condition observed in *N. megamastoides* from Villarroya and from Perrier-Les Etouaires. In tooth morphology, the shape of the upper molars is intermediate between the buccolingually wide teeth of *N. tingi* and the narrower ones of derived species like *N. sinensis* or *N. megamastoides*; the cingulum that bounds the upper molar is better developed compared to that of *N. donnezani* from Perpignan and Layna. The majority of the recovered M1 (83%) possesses expanded and cusp-like mesial cingulum. Furthermore, the M2 paracone is larger than the metacone like in *N. megamastoides* or *N. vulpinus*. It also possesses a large and prominent M2 metaconule connected by the postprotocrista to the protocone, unlike the specimens of *N. tingi* or *N. donnezani*. The ventral margin of the mandible is short rostrocaudally, and tend to be curved in contrast to the straight ventral margin of the other Eurasian species of *Nyctereutes* (e.g., *N. sinensis*, *N. megamastoides*). The presence of an evident cristid connecting the hypoconid and the entoconid on both the m1 (e.g., MNHN.F.ACA294 and MNHN.F.ACA549; 75% the preserved m1) from Çalta is unusual for *N. donnezani*, *N. tingi* or *N. sinensis* whereas is common in *N. megamastoides*

(see previous discussion). Moreover, the m1 metaconid of *Nyctereutes* from Çalta is rather prominent compared to that of *N. donnezani* from Perpignan and Layna, or even *N. tingi* and *N. sinensis* from China; it resembles that of *N. megamastoides* from e.g., from Dafnero or Kvabebi. In dental proportions, the sample from Çalta differs considerably from the Chinese species *N. tingi* and *N. sinensis* (Fig. 9A). More similarities can be found with the European taxa, especially with *N. megamastoides*, as shown in Fig. 9B. This mixed pattern of features, with resemblance and difference with various Eurasian taxa, makes the original attribution at least doubtful. For the moment, we therefore prefer referring the sample of Çalta as *Nyctereutes* sp.

In other localities of Southeastern and Eastern Europe, some scanty remains of fossil raccoon-dogs with primitive features have been described. Spassov (2003) reported *N. cf. tingi* from the Bulgarian site of Varshets (referred to the St. Vallier Faunal Unit, MN17), while the remains from Megalo Emvolon (Greece; MN15) was ascribed to *N. tingi* (Koufos, 1997). If the attributions were confirmed, these remains would extend the distribution of the Chinese species into Europe and, in the case of Varshets material, also in time (from 3 Ma to 2.2 Ma). The maxillary fragment recovered from Weze (Poland, MN15-16) originally described by Stach (1954) as *Nyctereutes* sp., was later referred to as *N. aff. donnezani* (Soria & Aguirre 1976) although some of the dental features of the specimen (e.g., the M1 and M2 are rather shortened buccolingually and these teeth tend to be quadrangular in occlusal shape; the M2 has a larger paracone compared to the metacone) resemble more those of *N. megamastoides* of Perrier-Les Etouaires and Dafnero. A reinterpretation of these fossils in the biogeographic framework of the raccoon-dog evolutionary history would hopefully provide new evidence to solve some of the above-mentioned issues.

Historically the appearance of derived species of *Nyctereutes* in Western Europe, namely *N. megamastoides*, has been referred to the Late Pliocene, around 3 Ma (Bartolini Lucenti 2017) and no record of co-occurrence of primitive and derived taxa in European localities is reported in the literature. This contrast with the Eastern Asian record of the Yushe Basin, in which *N. tingi* coexists with *N. sinensis* (Tedford & Qiu 1991). The recognition of *N. megamastoides* within the sample of Layna un-

Fig. 9 - Log-ratio diagrams on selected upper and lower teeth variables in *Nyctereutes* from Çalta as compared to the extant *N. procyonoides* (used as the reference baseline) and to *N. tingi* and *N. sinensis* (A) and to *N. donnezani*, *N. vulpinus* and *N. megamastoides* (B). The extant *N. procyonoides* is used as the reference baseline in both diagrams.



veils an unexpected ecological pattern in a European site similar to the correspondent to the Chinese one. This discovery reveals that the earliest arrival of *N. megamastoides*-like raccoon-dogs in Europe was much earlier than previously thought, around 3.9 Ma (Domingo et al. 2013). Furthermore, it is remarkable that in dental morphology these specimens resemble the younger *N. megamastoides* recovered from other European sites, e.g., Kvabebi, Lower Valdarno, Dafnero. The discovery of the derived taxon *N. megamastoides* in such an early site forces us to reevaluate the paradigms of dispersion and evolution of this taxon and more in general of all the Eurasian raccoon-dogs. For instance, the generally accepted hypothesis for the origin of *N. megamastoides*, as the result of anagenetic evolution from *N. donnezani*, seems less likely as the two appeared more or less contemporarily and apparently coexisted in the Spanish site. The alleged homology between *N. sinensis* and *N. megamastoides* based on shared derived features and the view of such species as a single taxon with a large paleobiogeographic

range, favored by Tedford & Qiu (1991), could contrast with the scenario suggested by the discovery of *N. megamastoides* at Layna. With its peculiar derived morphology, the latter species probably evolved in Eurasia more or less contemporarily to and independently from the *N. sinensis* lineage. Moreover, the characterizing cranial and dentognathic features of *N. sinensis* remain stable throughout the Yushe Basin Pliocene succession. Morphometric and morphological evidence might suggest a closer affinity between *N. sinensis* and *N. vulpinus*. This reinterpretation of the dispersal pattern and evolutionary history of Pliocene species, allows us to reconsider the specimens from Çalta. Their size, the mosaic pattern of primitive and derived features, but different from *N. donnezani* and *N. tingi*, combined with the similarity in dental proportions to *N. megamastoides*, are elements that suggest the possible presence of an unknown lineage, parallel to that of *N. tingi*-*N. donnezani*, and which eventually lead to the appearance of *N. megamastoides* in Eurasia.

Thanks to the method of the molar ratio in-

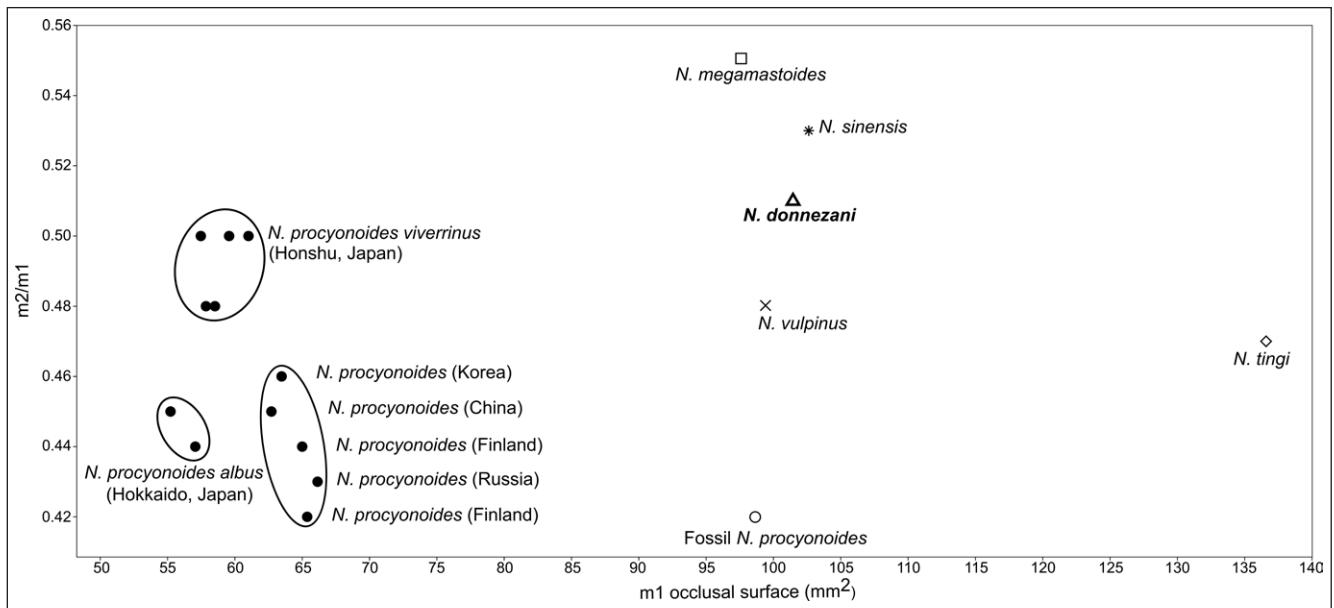


Fig. 10 - Biplot of the $m2/m1$ scores against the $m1$ occlusal surface (in mm^2) in various species and subspecies of *Nyctereutes* (see Materials and Methods for details). Fossil species are represented by average values. Black circles represent extant taxa; the open circle represents Chinese fossil *N. procyonoides*-like forms from Zhoukoudian loc. 1 (Pei 1934) and Renzidong (Jin & Liu 2009) [$n=7$]; asterisk represents *N. sinensis* from the Yushe Basin (China) [$n=22$]; open square represents *N. megamastoides* (from Kvabebi, Georgia and Senéze, France) [$n=5$]; X represents *N. vulpinus* from St. Vallier (France) [$n=8$]; open triangle represents *N. donnezani* (from Perpignan, La Gloria 4 and Layna) [$n=7$]; plus represents *N. tingi* from Yushe Basin (China) [$n=4$]. Updated from Bartolini Lucenti (in press).

Asahara & Takai (2016) showed that *Nyctereutes* spp. and ssp. possess a certain degree of dietary plasticity. Based on this method applied to the considered sample, we calculated a new score for the species *N. donnezani* ($m2/m1 = 0.482$), different from that known in literature (Fig. 10). The resulting mean score for *N. donnezani* (0.51) is slightly above the range of variability of the extant *N. procyonoides viverrinus* (Temminck, 1838) from Honshu (Japan), whereas it is higher than that of *N. tingi* (0.48) and of other living subspecies of *N. procyonoides*. This suggests that *N. donnezani*, as well as *N. tingi*, had a diet comparable to that of *N. p. viverrinus* (omnivorous, see Asahara & Takai 2016), although it does not show such a set of derived features in the mandible as extant raccoon-dogs. The mean molar ratio score of *N. vulpinus* from St. Vallier ($m2/m1 = 0.48$) testify to different dietary preferences in comparison to *N. megamastoides* or *N. sinensis*. Indeed, in the French species, the subangular lobe is moderately developed but the dental morphology is suggestive of a more carnivorous diet compared to taxa like *N. megamastoides* or *N. sinensis*, in which their dental dimensions and morphologies suggest slightly different diet adaptations. Peculiar among the fossil species *N. vulpinus* may suggest similar niche occupation.

The study of the fossil record shows that the different *Nyctereutes* species have developed dentogonatic features to progressively take advantage of a great variety of food items from the earlier species as *N. tingi* and *N. donnezani* to more recent ones as *N. megamastoides* and *N. sinensis*. The former possess characteristics suggestive of meso- to hypocarnivorous diet. The latter, with shared or similar morphologies to the extant *N. procyonoides*, show a shift in diet a hypocarnivorous diet. The enlargement and development of the crushing parts of teeth (both upper and lower) against slicing parts (see also Soria & Aguirre 1976; Tedford & Qiu 1991; Rook et al. 2017), the higher molar ratios (Fig. 10), etc. are all evidence of this dietary specialization. It is not clear which of the fossil species is the direct ancestor of *N. procyonoides* (although some scholars deem *N. sinensis* as the most probable), it is clear that it retains derived mandibular and dental features typical of this clade. Nevertheless, the morphological and morphometric evidence on this species and this subspecies (e.g., the molar ratio index or the elongation and buccolingual compression of lower molars compared to some fossil taxa) suggests an inversion of the trend towards an effective hypocarnivorous diet and that the spectrum of dietary preferences widened toward a greater plasticity in their diet.

In conclusion, the description of the new raccoon-dog material recovered at Layna improves our knowledge on the primitive-like species *N. donnezani*, thanks to the discovery of a nearly complete although damaged cranium (MNCN-63662) and several postcranial elements. Furthermore, the study of this sample pointed out the presence of few specimens that do not show the diagnostic features of *N. donnezani*. The morphological and morphometric comparisons of these fossils strongly support an affinity to the derived species *N. megamastoides*, and we therefore referred them to as *N. cf. megamastoides*. This represents the earliest known record of a derived species in Western Europe, backdating its appearance of nearly one Ma. Surely, this record, combined with that of Çalta, opens new questions regarding the origin of derived species of raccoon-dogs and has strong implications for our understanding of the pattern of evolution and dispersal of these species around the Old World.

Acknowledgements. The authors are thankful to the kindness and availability of E. Cioppi and P. Agnelli, curators of the IGF and of the MZUF, respectively; M. Bukhsianidze of the GNM; E. Robert of the “Laboratoire de Géologie”, Université Claude-Bernard-Lyon-1; D. Berthet of the Musée des Confluences; J. Galkin and J. Meng, for granting access to the collection of fossil mammals of AMNH; M. Gasparik, curator of the Palaeovertebrate Collection of the HMNH; C. Argot, from the Palaeovertebrate collection of the MNHN. The critical remarks of R. Sardella and two anonymous reviewers are deeply acknowledged, they were crucial to substantially improve the originally submitted manuscript. This research has been partly supported by the SYNTHESYS Project <http://www.synthesys.info/> (Project Numbers ES-TAF-6553, HU-TAF-6520 to SBL), which is financed by European Community Research Infrastructure Action under the FP7 “Capacities” Program. The Spanish Research Project CGL2015-68333-P (MINECO/FEDER-UE) and the Research Groups CSIC 641538 and CAM-UCM 910607 funded aspects of this research.

REFERENCES

- Aguirre E., Hoyos M., Mensua S., Morales J., Pérez González A., Quirantes J., Sánchez L. & Soria D. (1974) - Cuenca del Jalón. In Aguirre E. & Morales J. (Eds) - Libro-Guía del Coloquio Internacional sobre Biostratigrafía Continental del Neógeno superior y Cuaternario inferior: 13-45, CSIC, Madrid.
- Aguirre E., Morales J. & Soria D. (1981) - Accumulated bones in a Pliocene cave in Cerro Pelado, Spain. *Natl. Geogr. Soc. Res. Rep.*, 13: 69-81
- Alcalá-Martínez L. (1994) - Macromamíferos neógenos de la fosa de Alfambra-Teruel. PhD Thesis; Teruel: Museo Nacional de Ciencias Naturales, 554 pp.
- Argant A. (2004) - Les Carnivores du gisement Pliocène final de Saint-Vallier (Drôme, France). *Geobios*, 37: 133-182.
- Asahara M. (2013) - Shape variation in the skull and lower carnassial in a wild population of raccoon-dog (*Nyctereutes procyonoides*). *Zool. Sc.*, 30: 205-210.
- Asahara M. (2014) - Evolution of relative molar sizes among local populations of the raccoon dog (*Nyctereutes procyonoides*) in Japan. *Mammal Study*, 39: 181-184. <https://doi.org/10.3106/041.039>.
- Asahara M. & Takai M. (2016) - Estimation of diet in extinct raccoon-dog species by the molar ratio method. *Acta Zool.* (Stockholm), 98: 1-8.
- Asahara M., Saito K., Kishida T., Takahashi K. & Bessho K. (2016) - Unique pattern of dietary adaptation in the dentition of Carnivora: Its advantage and developmental origin. *Proc. R. Soc. B*, 282: 20160375.
- Bartolini Lucenti S. (in press) - “Measure my teeth and you will know what I ate”: The molar ratio method and an updated interpretation of the diet of *Nyctereutes sinensis* (Carnivora, Canidae). *Acta Zool.* (Stockholm). <https://doi.org/10.1111/azo.12232>
- Bartolini Lucenti S. (2017) - *Nyctereutes megamastoides* (Canidae, Mammalia) from the early and middle Villafranchian (late Pliocene and early Pleistocene) of the Lower Valdarno (Firenze and Pisa, Tuscany, Italy). *Riv. It. Paleontol. Strat.*, 123: 211-218.
- Bartolini Lucenti S. (2018) - *Nyctereutes* Temminck, 1838 (Mammalia, Canidae): a revision of the genus across the Old World during Plio-Pleistocene times. *Fossilia*, Vol. 2018: 7-10.
- Bernor R.L. & Sen S. (2017) - The Early Pliocene *Plesiohipparion* and *Proboscideipparion* (Equidae, Hipparionini) from Çalta, Turkey (Ruscinian Age, c. 4.0 Ma). *Geodiversitas*, 39: 285-314.
- Bowdich T.E. (1821) - An analysis of the natural classification of Mammalia for the use of students and travelers: J. Smith, Paris, 115 pp.
- Clauzon G., Le Strat P., Duvail C., Do Couto D., Suc J.P., Molliex S., Bache F., Besson D., Lindsay E.H., Opdyke N.D., Rubino J.L., Popescu S.-M., Haq B. U & Gorini C. (2015) - The Roussillon Basin (S. France): A case-study to distinguish local and regional events between 6 and 3 Ma. *Mar. Pet. Geol.*, 66: 18-40.
- Del Campana D. (1913) - I cani pliocenici di Toscana. *Palaeontogr. Ital.*, 19: 189-254.
- Depéret C. (1890) - Les Animaux Pliocènes du Roussillon. *Mém. Soc. Géol. Fr.*, 3: 5-195.
- Domingo M. S., Alberdi M. T. & Azanza B. (2007) - A new quantitative biochronological ordination for the Upper Neogene mammalian localities of Spain. *Palaeogeogr., Palaeoclimatol., Palaeoecol.*, 255: 361-376.
- Domingo L., Koch P.L., Fernández M.H., Fox D.L., Domingo M.S. & Alberdi M.T. (2013) - Late Neogene and early Quaternary paleoenvironmental and paleoclimatic conditions in southwestern Europe: isotopic analyses on mammalian taxa. *PLoS One*, 8: e63739.
- Driesch von den A. (1976) - A guide to the measurement of animal bones from archaeological sites. *Peabody Mus. Bull.*, 1: 1-137.
- Ficcarelli G., Torre D. & Turner A. (1984) - First evidence for a species of raccoon dog, *Nyctereutes* Temminck, 1838, in South African Plio-Pleistocene deposits. *Boll. Soc. Paleont. It.*, 23: 125-130.
- Fischer von Waldheim G. (1817) - Adversaria Zoologica. *Mem. Soc. Imp. Nat. Mosc.*, 5: 368-428.
- Frisch J.L. (1775) - Das Natur-System der vierfüßigen Thiere in Tabellen, darinnen alle Ordnungen, Geschlechter und Arten, nicht nur mit bestimmenden Benennungen, sondern beygesetzten unterscheidenden Kennzeichen angezeigt werden zum Nutzen

- der erwachsenen Schuljugend: C. F. Günther, Glogau: 1-30.
- García N. & Arsuaga J.L. (1999) - Carnivores from the early Pleistocene hominid bearing Trinchera Dolina 6 (Sierra de Atapuerca, Spain). *J. Hum. Evol.*, 37: 415-430.
- Geraads D., Alemseged Z., Bobe R. & Reed D. (2010) - *Nyctereutes lockwoodi*, n. sp., a new canid (Carnivora: Mammalia) from the middle Pliocene of Dikika, Lower Awash, Ethiopia. *J. Vert. Paleont.*, 30, 981-987.
- Ginsburg L. (1998) - Le gisement de vertébrés pliocènes de Çalta, Ankara, Turquie. 5. Carnivores. *Geodiversitas*, 20: 379-396.
- Gray J. (1834) - Illustration of Indian zoology, consisting of coloured plates of new or hitherto unfigured Indian animals from the collection of Major General Hardwicke: Treuttell, Wurtz, Treuttell, Richter Publishers, London, 2, 203 pp.
- Hammer Ø., Harper D.A.T. & Ryan P.D. (2001) - PAST: Paleontological statistics software package for education and data analysis. *Palaeontol. Electron.*, 4: art. 4.
- Hammer Ø. (2016) - PAST: PAleontological STatistics. Version 3.14. Reference manual: Natural History Museum, University of Oslo. <http://folk.uio.no/ohammer/past/past3manual.pdf>.
- Hartstone-Rose A., Kuhn B.F., Nalla S., Werdelin L. & Berger L.R. (2013) - A new species of fox from the *Australopithecus sediba* type locality, Malapa, South Africa. *Trans. R. Soc. S. Afr.*, 68: p. 1-9.
- Hemmer H., Kahlke R.-D. & Vekua A. (2004) - The Old World puma - *Puma pardoides* (Owen, 1846) (Carnivora: Felidae) - in the Lower Villafranchian (Upper Pliocene) of Kvabebi (East Georgia, Transcaucasia) and its evolutionary and biogeographical significance. *Neues Jahrb. Geol. Paläontol.*, 233: 197-231.
- Hemprich F. W. & Ehrenberg C.G. (1832) - Symbolae Physicae. Mammalia: Ex Officina Academica, 2. Berlin.
- Hornaday W. T. (1904) - A new species of raccoon dog. *Ann. Rep. New York Zool. Soc.*, 8: 71-73.
- Hoyos M., Soler V., Rodríguez E., Carracedo J.C. & Chicharro P.M. (1987) - Posición magnetoestratigráfica de los yacimientos de vertebrados neógenos de Algorta y Layna (Cordillera Ibérica). Reunión de Paleomagnetismo. Arenys de Mar, Spain.
- Kavanagh K.D., Evans A.R. & Jernvall J. (2007) - Predicting evolutionary patterns of mammalian teeth from development: *Nature*, 449: 427-432.
- Koufos G.D. (1997) - The canids *Eucyon* and *Nyctereutes* from the Ruscinian of Macedonia, Greece. *Paleontol. Evol.*, 30/31: 39-48.
- Koufos G.D. (2014) - The Villafranchian carnivoran guild of Greece: implications for the fauna, biochronology and paleoecology. *Integr. Zool.*, 9: 444-460.
- Kretzoi M. (1943) - *Kochictis centenii* n. g. n. sp., ein altertümlicher Creodonte aus dem Oberoligozän Siemenbürgens. *Földtany Közlöny*, 52: 190-195.
- Linnaeus C. (1758) - Systema Naturae per regna tria naturae, secundum Classes, Ordines, Genera, Species, cum characteribus, differentiis, synonymis, locis. Tomus I, 10th edition: Holmiae, Laurentius Salvius, Stockholm, Sweden, 824 pp.
- López-Martínez N. (1989) - Revisión sistemática y bioestratigráfica de los Lagomorpha (Mammalia) del Terciario y Cuaternario de España. *Mem. Mus. Paleontol. Univers. Zaragoza*, 3:5-343.
- Martin R. (1971) - Les affinités de *Nyctereutes megamastoides* (Pomel), Canidae du gisement villafranchien de Saint-Vallier (Drôme, France). *Palaeovertebrata*, 4: 39-58.
- Monguillon A., Spassov N., Argant A., Kauhala K. & Viranta S. (2004) - *Nyctereutes vulpinus* comb. et stat. nov. (Mammalia, Carnivora, Canidae) du Pliocène terminal de Saint-Vallier (Drôme, France): *Géobios*, 7: 83-88.
- Morales J. (2016) - Los carnívoros de Villarroya. In: Alberdi Alonso M.T., Azanza Asensio B. & Cervantes E. (Eds) - Villarroya, yacimiento clave de la paleontología riojana: 119-142.
- Pérez B. & Soria D. (1989-90) - Análisis de las comunidades de mamíferos del Plioceno de Layna (Soria) y La Calera (Teruel). *Paleontol. Evol.*, 23: 231-238.
- Pomel M. (1842) - Nouvelle espèce de chien fossile découverte dans les alluvions volcaniques de l'Auvergne. *Bull. Soc. Géol. Fr.*, 14: 38-41.
- Rook L., Bartolini Lucenti S., Bukhshianidze M. & Lordkipanidze D. (2017) - The Kvabebi Canidae record revisited (late Pliocene, Sighnaghi, eastern Georgia). *J. Paleontol.*, 91: 1258-1271.
- Schlosser M. (1903) - Die fossilen Säugethiere Chinas nebst einer Odontographie de recenten Antilopen. *Abhandl. Bayer. Akad. Wiss.*, 22: 1-220.
- Sesé C. (2006) - Los roedores y lagomorfos del Neógeno de España. *Estudios Geológicos*, 62: 429-480.
- Simpson G.G. (1941) - Large Pleistocene felines of North America. *Am. Mus. Novit.*, 1136: 1-27.
- Simpson G.G., Roe A. & Lewontin R.C. (1960) - Quantitative Zoology: Harcourt Brace, New York, 440 pp.
- Smith C. H. (1839) - The Canine Family in general or the genus *Canis*. In: Jardine W. (Ed.) - The naturalist's library, vol. 18. Natural history of dogs, vol. 1. Edinburgh: W. H. Lizars, 267 pp.
- Soria D. & Aguirre E. (1976) - El cánido de Layna: revisión de los *Nyctereutes* fósiles. *Trabajos Neógeno y Cuaternario*, 5: 83-115.
- Spassov N. (2003) - The Plio-Pleistocene vertebrate fauna in South-Eastern Europe and the megafaunal migratory waves from the east to Europe. *Rev. Paléobiol.*, 22: 197-229.
- Stach J. (1954) - *Nyctereutes* (Canidae) w pliocenie Polski, Studia nad trzeciorzędową fauną brekcyj kostnej w miejscowości Węże koło Działoszyna. *Acta Geol. Pol.*, 4: 191-206.
- Tedford R.H. & Qiu Z. (1991) - Pliocene *Nyctereutes* (Carnivora: Canidae) from Yushe, Shanxi, with comments on Chinese fossil raccoon-dogs. *Vert. PalAs.*, 29: 176-189.
- Tedford R.H., Taylor B. & Wang X. (1995) - Phylogeny of the Caninae (Carnivora: Canidae): the Living Taxa. *Am. Mus. Novit.*, 3146: 1-37.
- Tedford R.H., Wang X. & Taylor B.E. (2009) - Phylogenetic systematics of the North American fossil caninae (Carnivora: Canidae). *Bull. Am. Mus. Nat. Hist.*, 325: 1-218.
- Teilhard de Chardin P. & Pivetau J. (1930) - Les mammifères fossiles de Nihewan (Chine). *Ann. Paleontol.*, 19: 1-134.
- Teilhard de Chardin P. & Pei W.-C. (1941) - The fossil mammals from Locality 13 of Choukoutien. *Palaeont. Sinica*, n. s. C., 11, 106 pp.
- Temminck C. (1838) - Over de kennis en de Verbreiding der Zoogdieren van Japan. *Tijdschr. Nat. Gesch. Phys.*, 5: 273-293.
- Viret J. (1954) - Le loess à bancs durcis de Saint-Vallier (Drôme) et sa faune de mammifères villafranchiens. *Nouv. Arch. Mus. Hist. Nat. Lyon*, 4: 1-200.
- Wayne R.K. & Ostrander E. A. (2007) - Lessons learned from the dog genome. *Trends Genet.*, 23: 557-567.
- Wayne R.K., Geffen E., Girman D.J., Koepfli K.P., Lau L.M. & Marshall C.R. (1997) - Molecular systematics of the Canidae. *Syst. Biol.*, 46: 622-653.